Geophysical Fluid Dynamics: from the Lab, up and down!

Henri-Claude Nataf
Univ Grenoble Alpes / CNRS
Grenoble, France

Fluid Dynamics in Earth and Planetary Sciences
Kyoto, November 27-30, 2018

UNIVERSITÉ Grenoble Alpes

cnrs dépasser les frontières

Lecture 3
Core dynamics and the geodynamo

FDEPS

Kyoto, November 28, 2018

inspired by 20 years in the geodynamo team in Grenoble

present and past members of the geodynamo team

Outline

3. Core dynamics and the geodynamo

3.1. The Earth's magnetic field

The Earth's magnetic field

- Almost all we know about the Earth's core comes from observing the magnetic field it produces.
- Measurements of the direction of the magnetic field at the surface of the Earth were available before Colomb's expeditions (1492).
- Intensity measurements began during La Pérouse's expedition (1785), and became absolute measurements with Gauss (1832) (geomagnetism).
- Human-made artefacts such as baked clays record the ancient magnetic field back to ~5000 years BP (archeomagnetism).
- Lavas and sediments record the magnetic field that existed when they formed, back to 3.45 Ga, arguably 4.2 Ga (paleomagnetism).

The historical magnetic field at the Earth's surface

- From compilations of navigators' logbooks, historical archives and observatory data (Jackson et al, 2000).

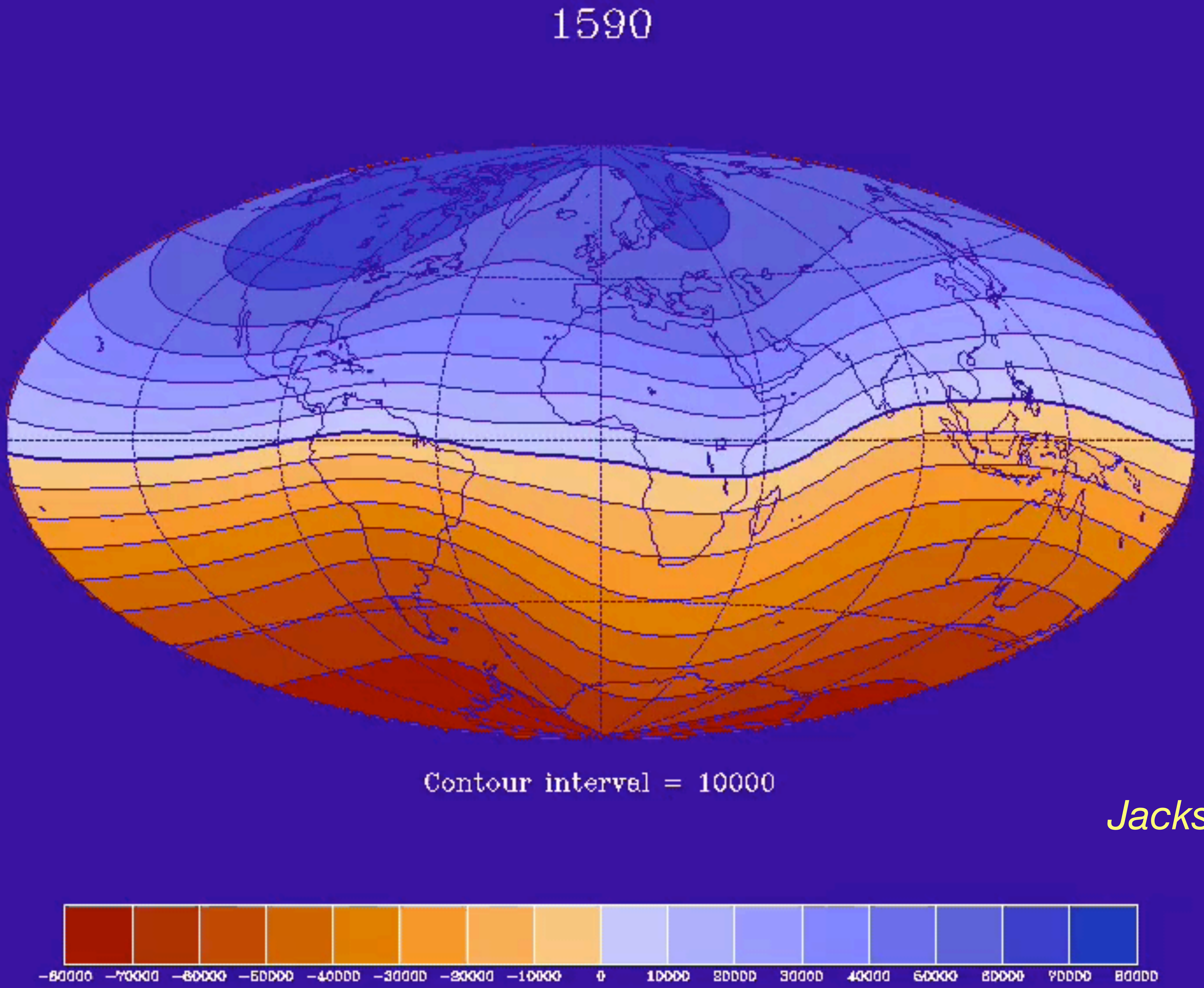

Jackson et al, 2000

Downward continuation of the magnetic field to the CMB

Assuming that the mantle is electrically insulating, one can continue the magnetic field from the Earth's surface down to the core-mantle boundary (CMB).

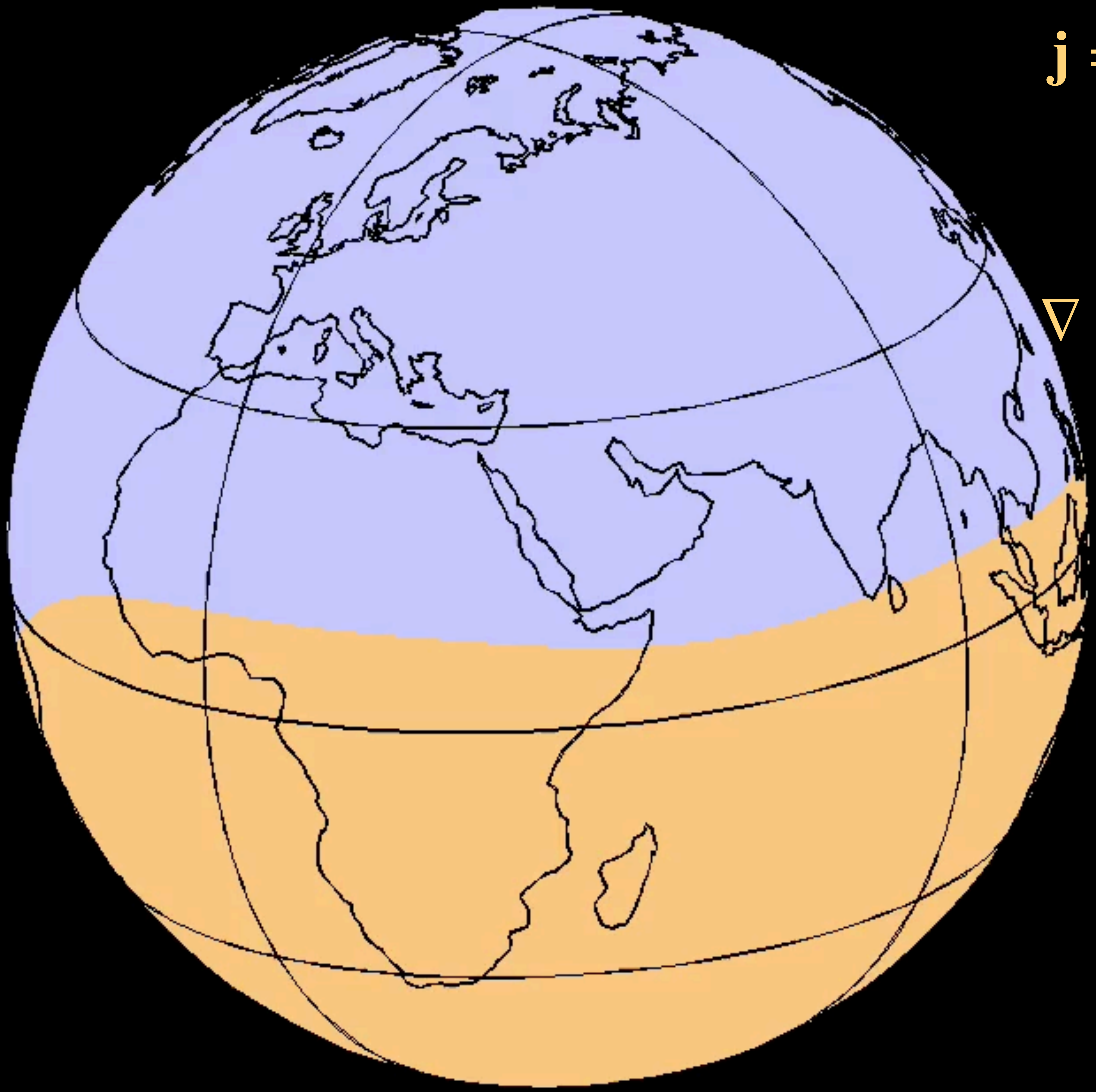

$$\mathbf{j} = \mathbf{0} \implies \nabla \times \mathbf{B} = \mathbf{0}$$

$$\mathbf{B} = \nabla \psi$$

$$\nabla \cdot \mathbf{B} = 0 \implies \nabla^2 \psi = 0$$

$$\implies \psi \sim \frac{1}{r^{l+1}}$$

Finlay & Jackson

The historical magnetic field at the CMB

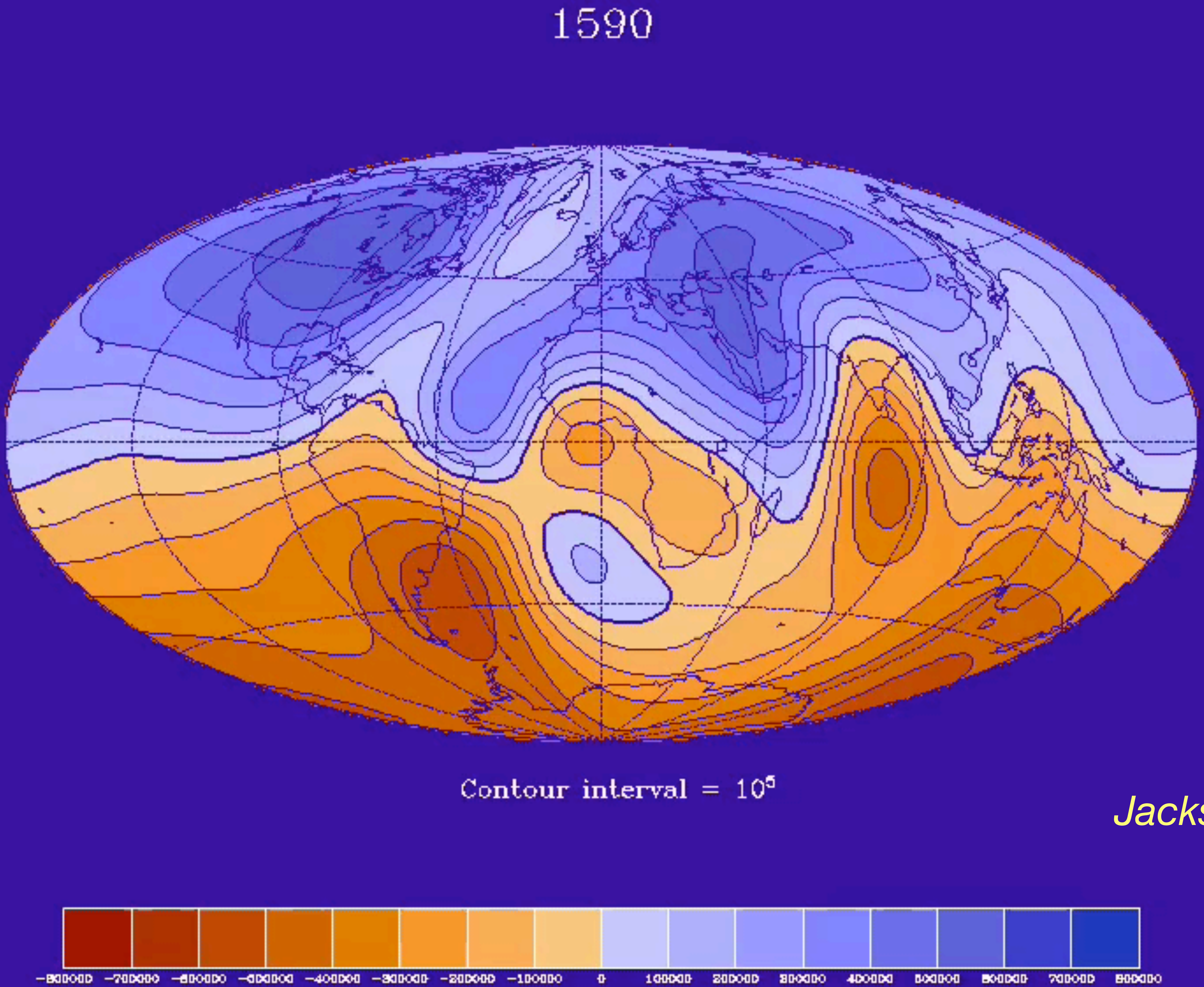

Jackson et al, 2000

The Holocene magnetic field at the CMB

- From archeomagnetic data and rapidly deposited lake sediments (Korte et al, 2000).

The Holocene magnetic field at the CMB

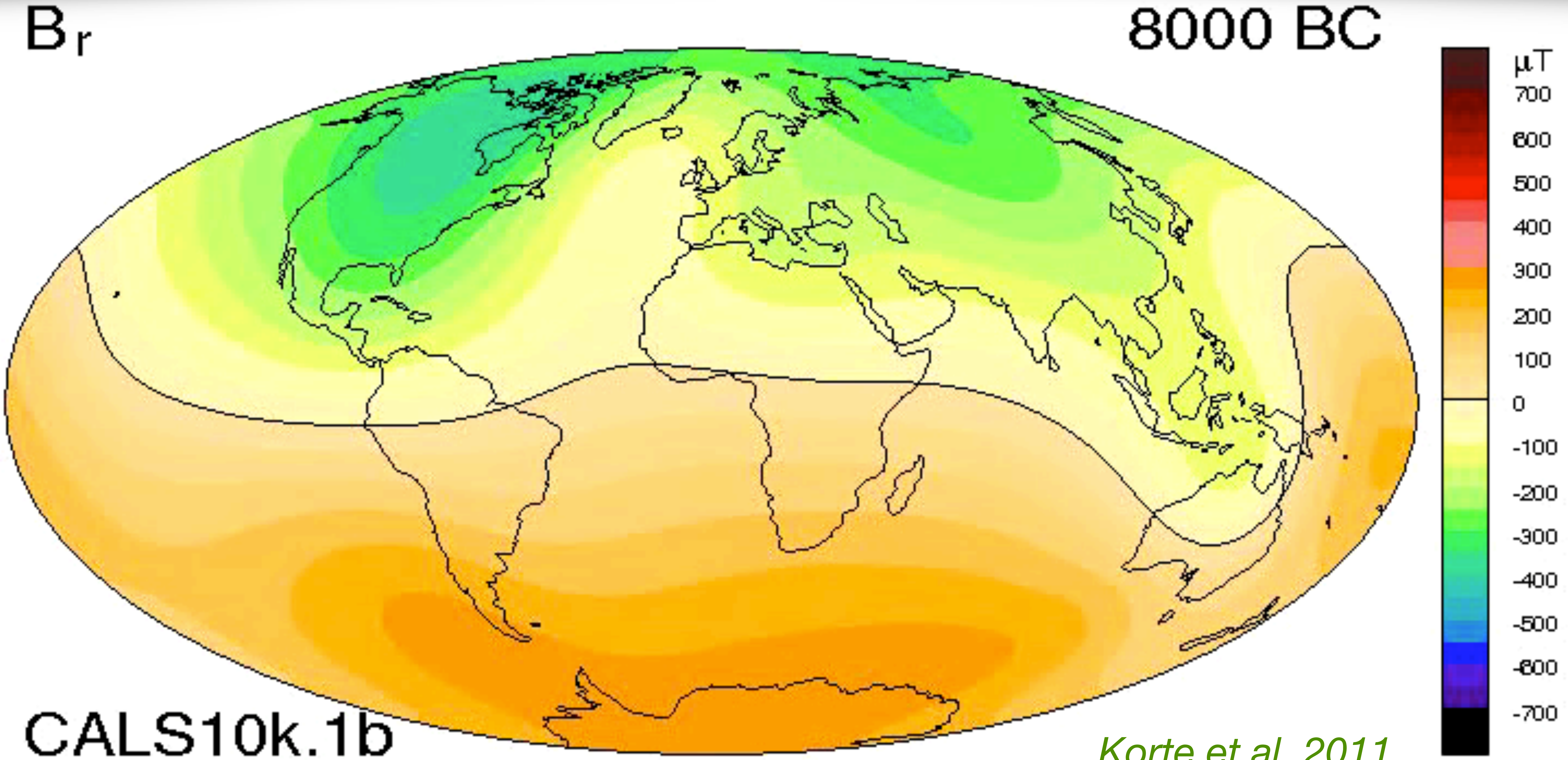

Korte et al, 2011

Magnetic intensity in the last 800,000 years

From IODP sedimentary cores (Tric et al, 1994).

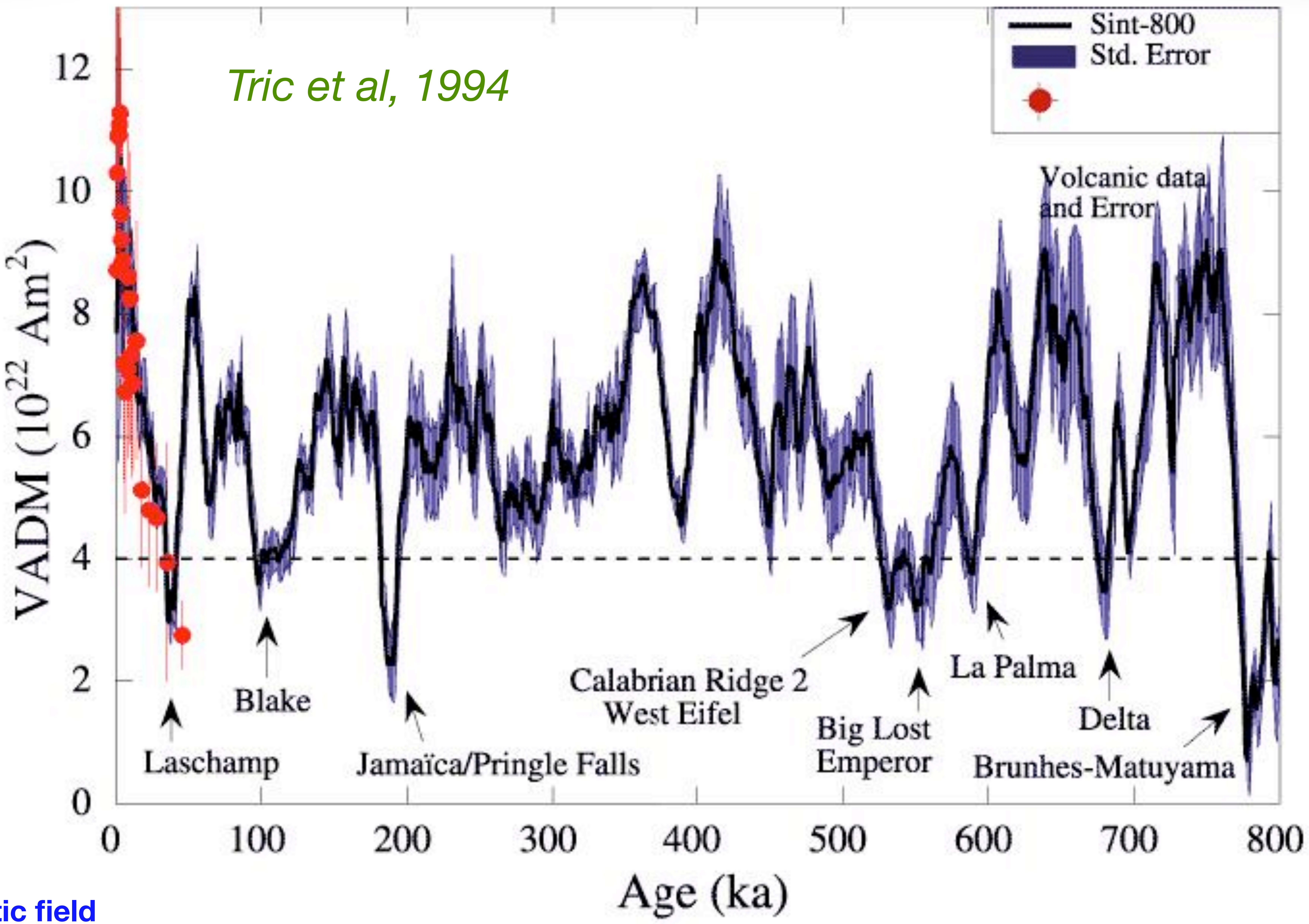

Magnetic field reversals from oceanic magnetic anomalies

- Magnetic anomalies over the North-Atlantic reveal many magnetic field reversals back to 180 Ma (extracted from the Magnetic Anomaly Map of the World, Korhonen et al, 2007).

Magnetic field reversals from oceanic magnetic anomalies

Magnetic field reversals in the geological history

GSA GEOLOGIC TIME SCALE v. 4.0

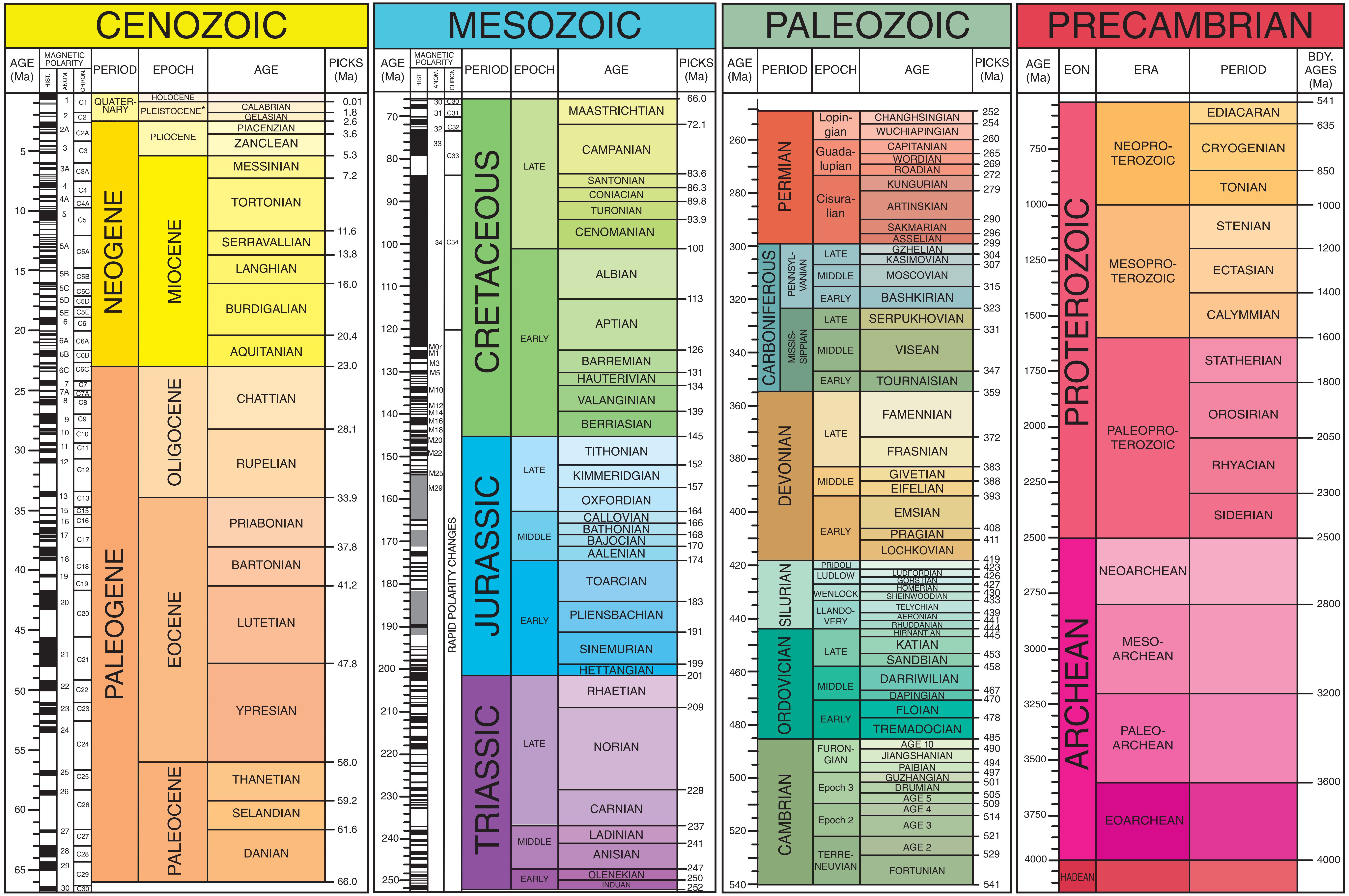

*The Pleistocene is divided into four ages, but only two are shown here. What is shown as Calabrian is actually three ages—Calabrian from 1.8 to 0.78 Ma, Middle from 0.78 to 0.13 Ma, and Late from 0.13 to 0.01 Ma.

Walker, J.D., Geissman, J.W., Bowring, S.A., and Babcock, L.E., compilers, 2012, Geologic Time Scale v. 4.0: Geological Society of America ... ©2012 The Geological Society of America.

The Cenozoic, Mesozoic, and Paleozoic are the Eras of the Phanerozoic Eon. Names of units and age boundaries follow the Gradstein et al. (2012) and Cohen et al. (2012) compilations. Age estimates and picks of boundaries are rounded to the nearest whole number (1 Ma) for the pre-Cenomanian, and rounded to one decimal place (100 ka) for the Cenomanian to Pleistocene interval. The numbered epochs and ages of the Cambrian are provisional.

THE GEOLOGICAL SOCIETY OF AMERICA®

Questions...

- How is the magnetic field produced in the Earth's core?
- Why is it mostly dipolar and aligned with the axis of rotation?
- Can we relate magnetic secular variation to motions in the core?
- Can we predict the future evolution of the magnetic field?
- What controls its intensity?
- What causes reversals?
- How long has the Earth had a magnetic field?

3.2. Dynamics of rotating fluids

Foreword

- In contrast with the mantle, the liquid core is a very low viscosity fluid. In fact, the kinematic viscosity of liquid iron at core conditions is expected to be about the same as water: **$\nu = 10^{-6}$ m²/s**.

- As in the atmosphere or the ocean, flow in the core is strongly affected by the **Coriolis force**, due to the Earth's spin.

- To decipher what happens in the core, and how the magnetic field is generated, it is essential to inject what we know of the **dynamics of rotating fluids**.

Outline

3.2. Dynamics of rotating fluids

3.2.1. Geostrophic equilibrium

The Navier-Stokes equation

- Let's recall the Navier-Stokes equation in the Boussinesq approximation:

$$\underbrace{\rho_0\left(\frac{\partial \mathbf{u}}{\partial t} + (\mathbf{u}\cdot\nabla)\mathbf{u}\right)}_{inertia} + \underbrace{2\rho_0 \boldsymbol{\Omega}\times\mathbf{u}}_{Coriolis} = \underbrace{-\nabla P}_{pressure} + \underbrace{\rho_0\left(1-\alpha(T-T_0)\right)\mathbf{g}}_{buoyancy} + \underbrace{\mathbf{j}\times\mathbf{B}}_{Lorentz} + \underbrace{\mu\nabla^2\mathbf{u}}_{viscous}$$

The Ekman number

- We have seen that the viscosity of the liquid is very small in the core. In the Navier-Stokes equation, a dimensionless number compares **viscous forces** to the **Coriolis force**. It is called the **Ekman number**, and can be written:

$$E = \frac{\nu}{\Omega r_o^2}$$

where Ω is the angular velocity of the rotating Earth, and r_o the radius of the core. Entering expected values, we find:

$$E \sim 10^{-15}$$

Hence, viscous forces should play a very limited role in the core.

The Rossby number

- The time-scale of the secular variation of the Earth's magnetic field (centuries) suggests flow velocities U of the order of a **mm/s** at most. The **Rossby number** compares **inertia** to the **Coriolis force**. We write it:

$$Ro = \frac{U}{\Omega r_o}$$

Plugging in our typical values, we get:

$$Ro \sim 10^{-6}$$

Hence, inertia should not be a major player either.

The geostrophic equilibrium

- We thus get:

$$\underbrace{\rho_0\left(\frac{\partial \mathbf{u}}{\partial t} + \cancel{(\mathbf{u}\cdot\nabla)\mathbf{u}}\right)}_{inertia} + \underbrace{2\rho_0\boldsymbol{\Omega}\times\mathbf{u}}_{Coriolis} = \underbrace{-\nabla P}_{pressure} + \underbrace{\rho_0\big(1-\alpha(T-T_0)\big)\,\mathbf{g}}_{buoyancy} + \underbrace{\mathbf{j}\times\mathbf{B}}_{Lorentz} + \underbrace{\cancel{\mu\nabla^2\mathbf{u}}}_{viscous}$$

- Ignoring buoyancy and the Lorentz force for the moment, the Navier-Stokes equation simplifies into the simple balance:

$$\underbrace{2\rho_0\boldsymbol{\Omega}\times\mathbf{u}}_{Coriolis} = \underbrace{-\nabla P}_{pressure}$$

- This is called the **geostrophic equilibrium**.

The geostrophic equilibrium

- The geostrophic equilibrium plays a major role for explaining motions in the atmosphere, the ocean, and the liquid core. It explains why winds circle around cyclones (typhoons) or depressions, rather than flowing from high to low pressure.

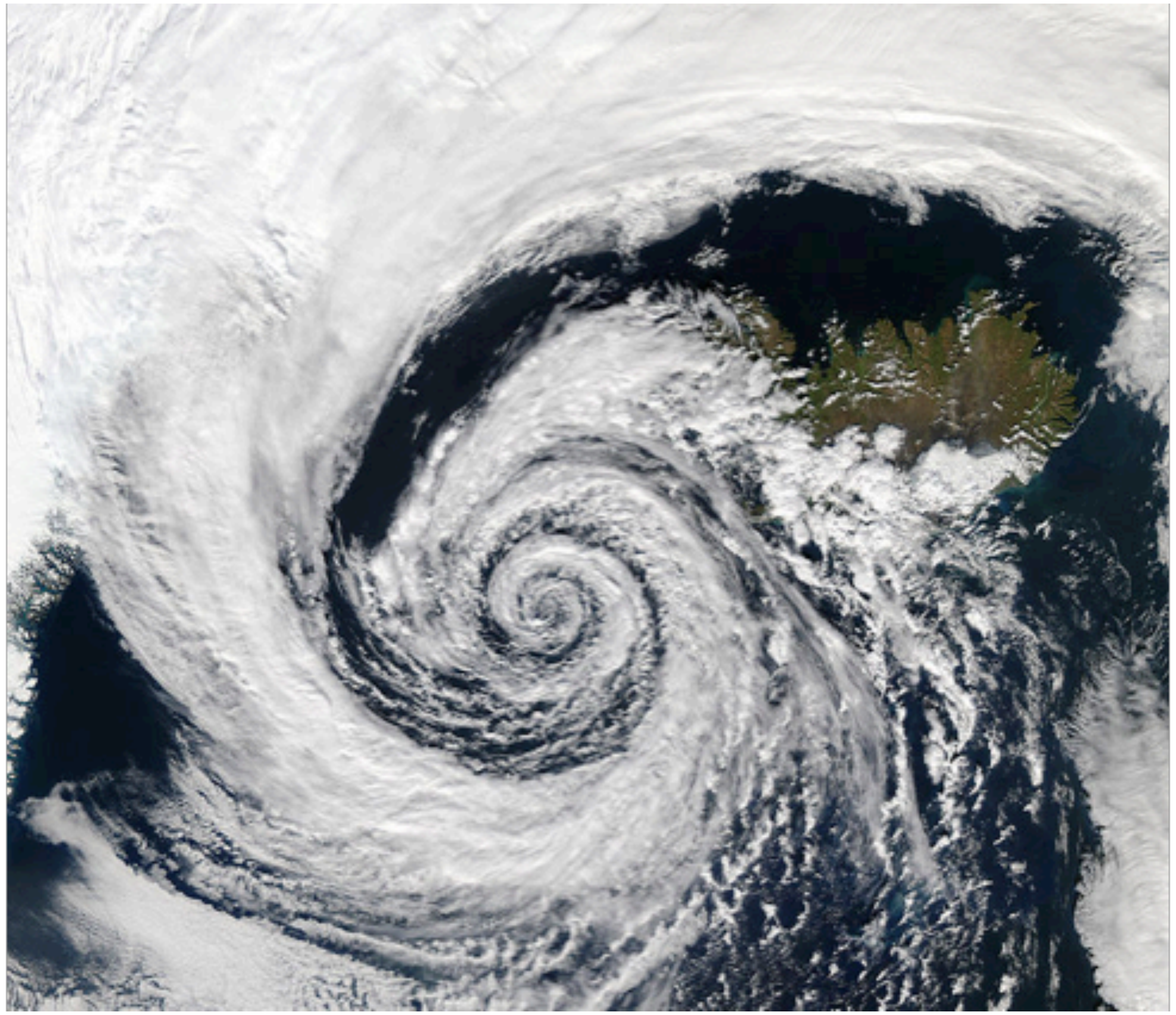

3.2.2. Taylor-Proudman theorem

Taylor-Proudman theorem

- The **Taylor-Proudman theorem** is a very powerful consequence of the geostrophic equilibrium. Take the curl of the geostrophic equation to eliminate the pressure term. You get:

$$(\nabla \cdot \mathbf{u})\,\hat{\mathbf{z}} - (\hat{\mathbf{z}} \cdot \nabla)\,\mathbf{u} = \mathbf{0}$$

where $\hat{\mathbf{z}}$ is the unit vector along the axis of rotation.

- For an incompressible fluid, this yields:

$$(\hat{\mathbf{z}} \cdot \nabla)\,\mathbf{u} = \mathbf{0}$$

meaning that **flow velocity is invariant along the axis of rotation.**

- A famous illustration of this property is given by the formation of a ‘phantom’ **Taylor column** above an obstacle in a rotating fluid

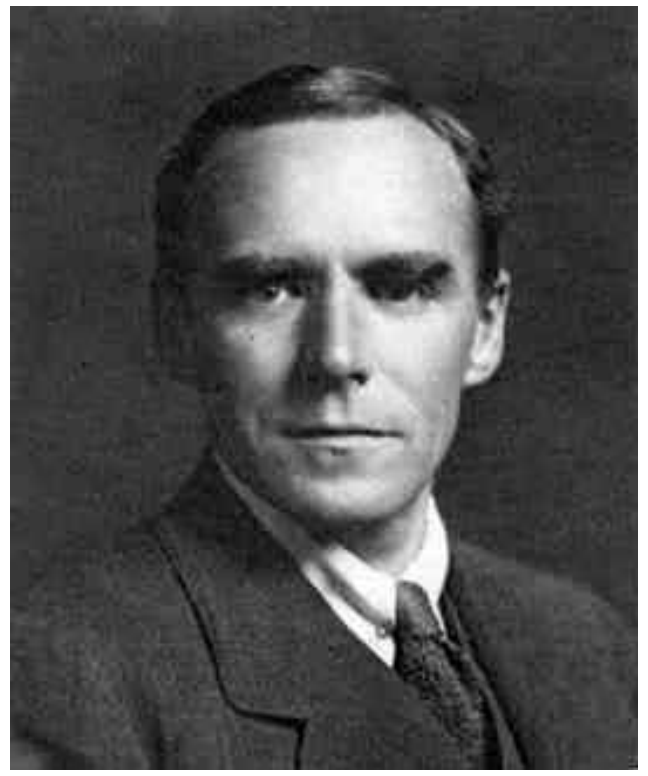

Geoffrey Taylor
(1886-1975)

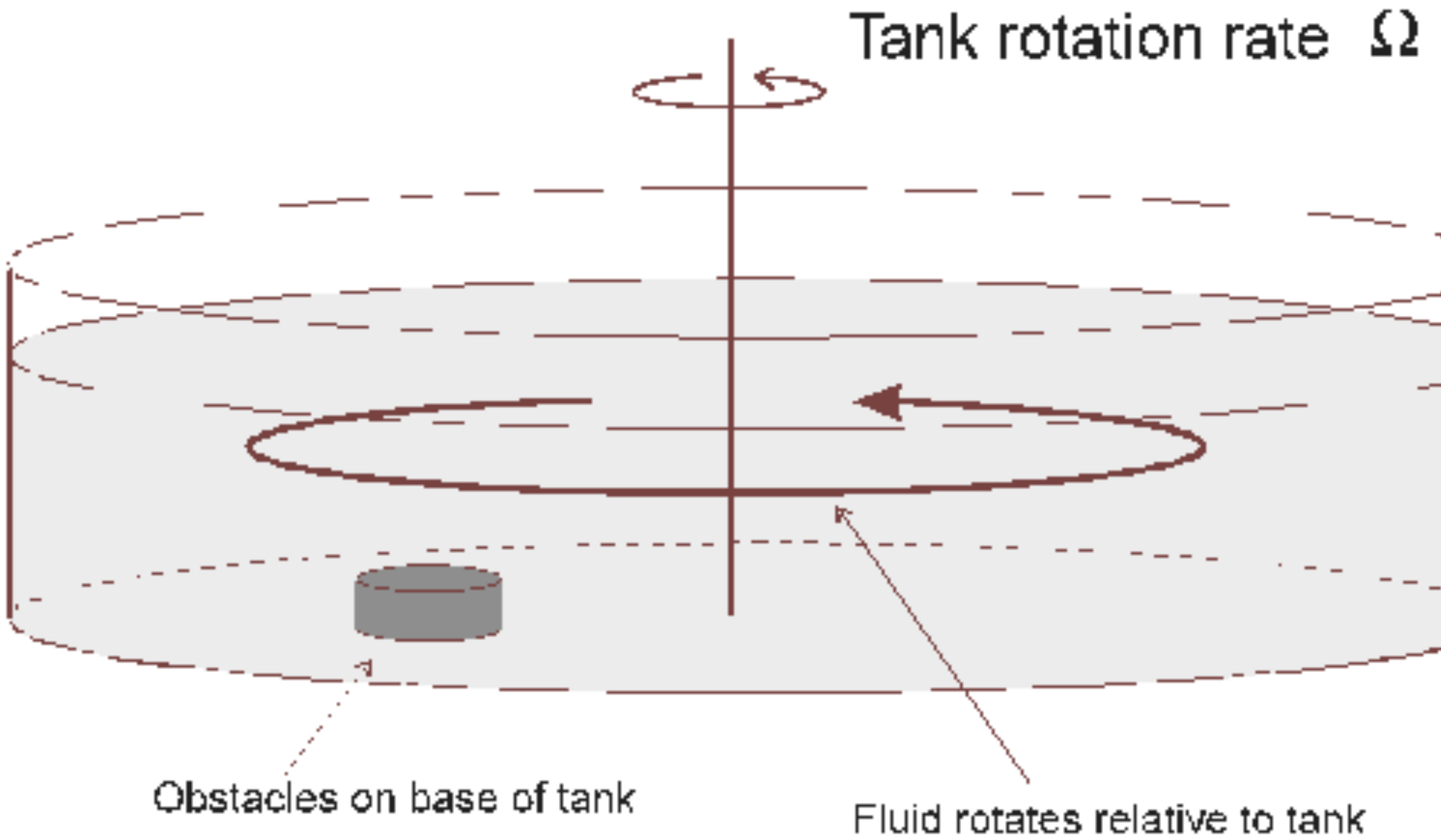

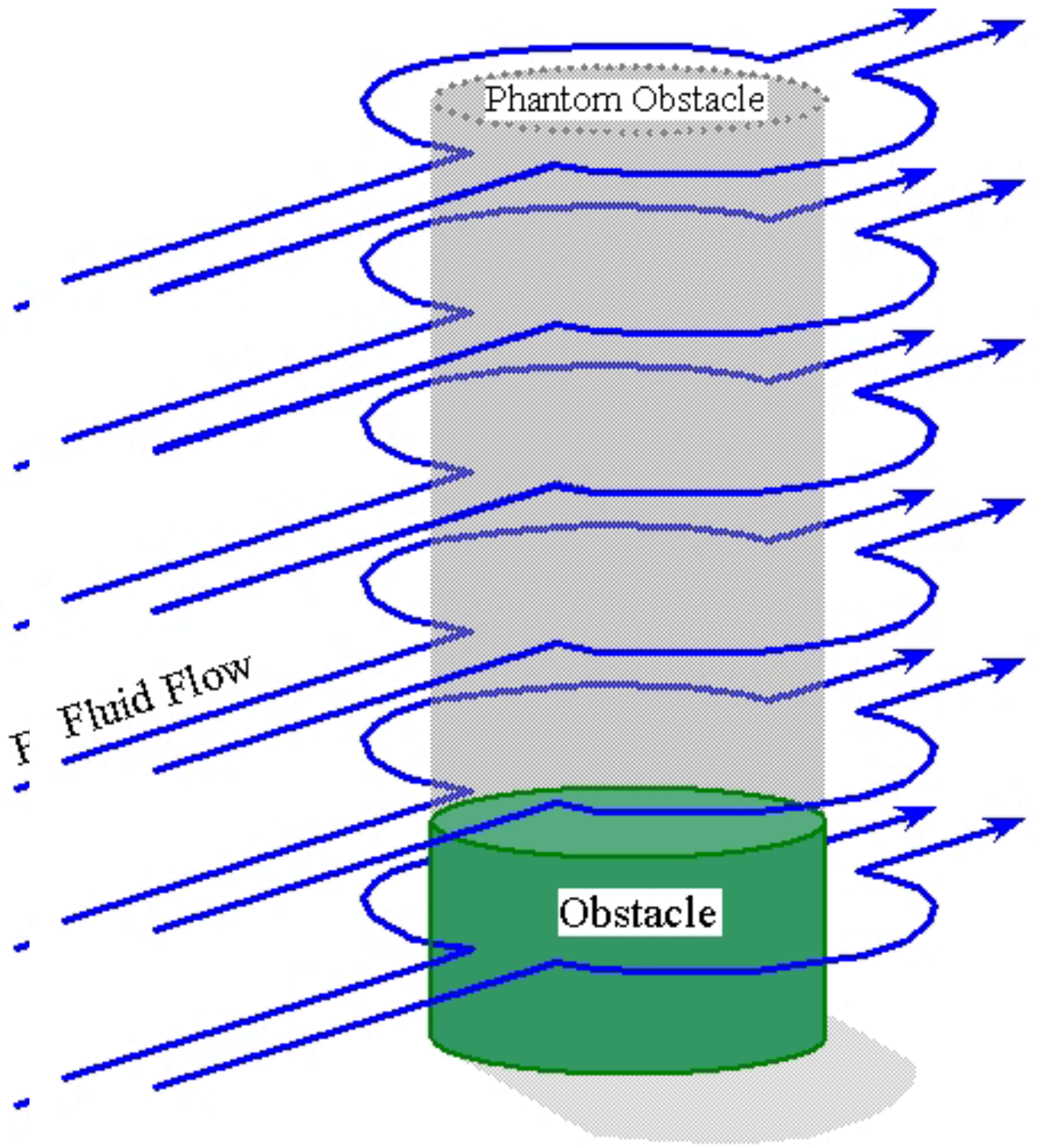

*from MITOPENCOURSEWARE: **GFDVII***

Taylor column experiment

3.2.3. Inertial waves

Inertial wave equation

- In a rotating fluid, the Coriolis force acts as a restoring force enabling the propagation of waves, called **inertial waves**.

- We restore the time-derivative term in the Navier-Stokes equation and get:

$$\frac{\partial \mathbf{u}}{\partial t} + 2\boldsymbol{\Omega} \times \mathbf{u} = -\frac{1}{\rho_0}\nabla P$$

- Taking the curl, we introduce the vorticity $\xi = \nabla \times \mathbf{u}$ and get:

$$\frac{\partial \xi}{\partial t} = -2\Omega\,(\hat{\mathbf{z}} \cdot \nabla)\mathbf{u}$$

- Taking the curl once more, applying a time derivative, we get:

$$\frac{\partial^2(\nabla \times \xi)}{\partial t^2} = 2\Omega\,(\hat{\mathbf{z}} \cdot \nabla)\frac{\partial \xi}{\partial t}$$

- Noting that $\nabla \times \xi = -\nabla^2 \mathbf{u}$, we finally get:

$$\frac{\partial^2 \nabla^2 \mathbf{u}}{\partial t^2} = -4\Omega^2 (\hat{\mathbf{z}} \cdot \nabla)^2 \mathbf{u}$$

- Plane wave solutions provide the dispersion relation:

$$\omega = \pm 2\Omega \frac{\hat{\mathbf{z}} \cdot \mathbf{k}}{k}$$

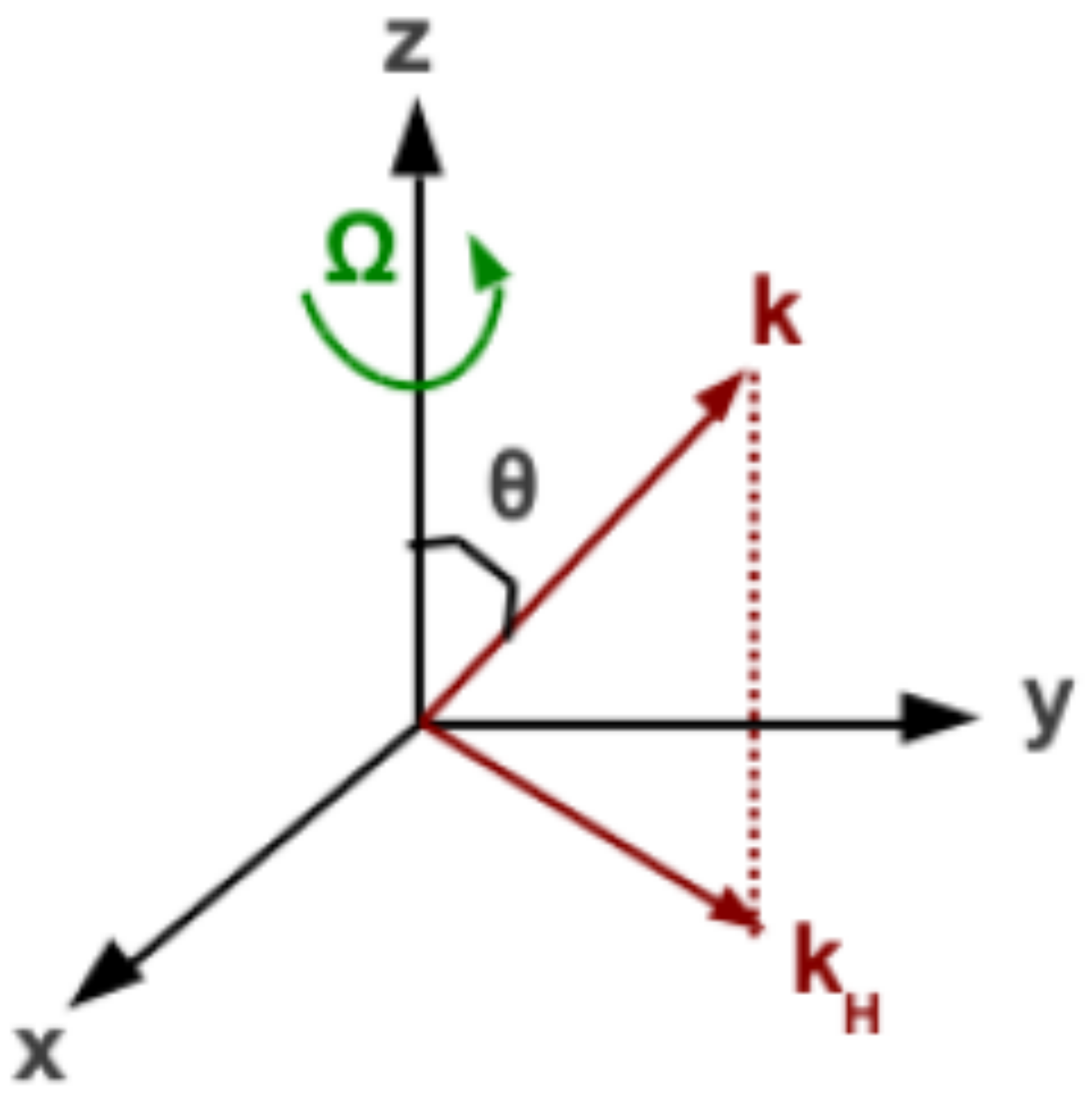

and the phase and group velocities:

$$c_\phi = \pm 2\Omega \frac{k_z}{k^2}$$

$$c_g = \pm 2\Omega \frac{\mathbf{k} \times (\hat{\mathbf{z}} \times \mathbf{k})}{k^3}$$

From lecture notes of Cébron and Vidal, 2017.

Inertial wave properties

- Inertial waves are transverse waves. Their pulsation is proportional to the cosine of the angle θ between their wave vector and the axis of rotation. Their maximum pulsation is 2Ω. Their phase propagates in a direction perpendicular to their energy. Geostrophic motions correspond to zero frequency inertial waves.

- Inertial waves can be excited by oscillating a small disk in a rotating tank.

- In a closed container, inertial waves build **inertial modes**.

(a)

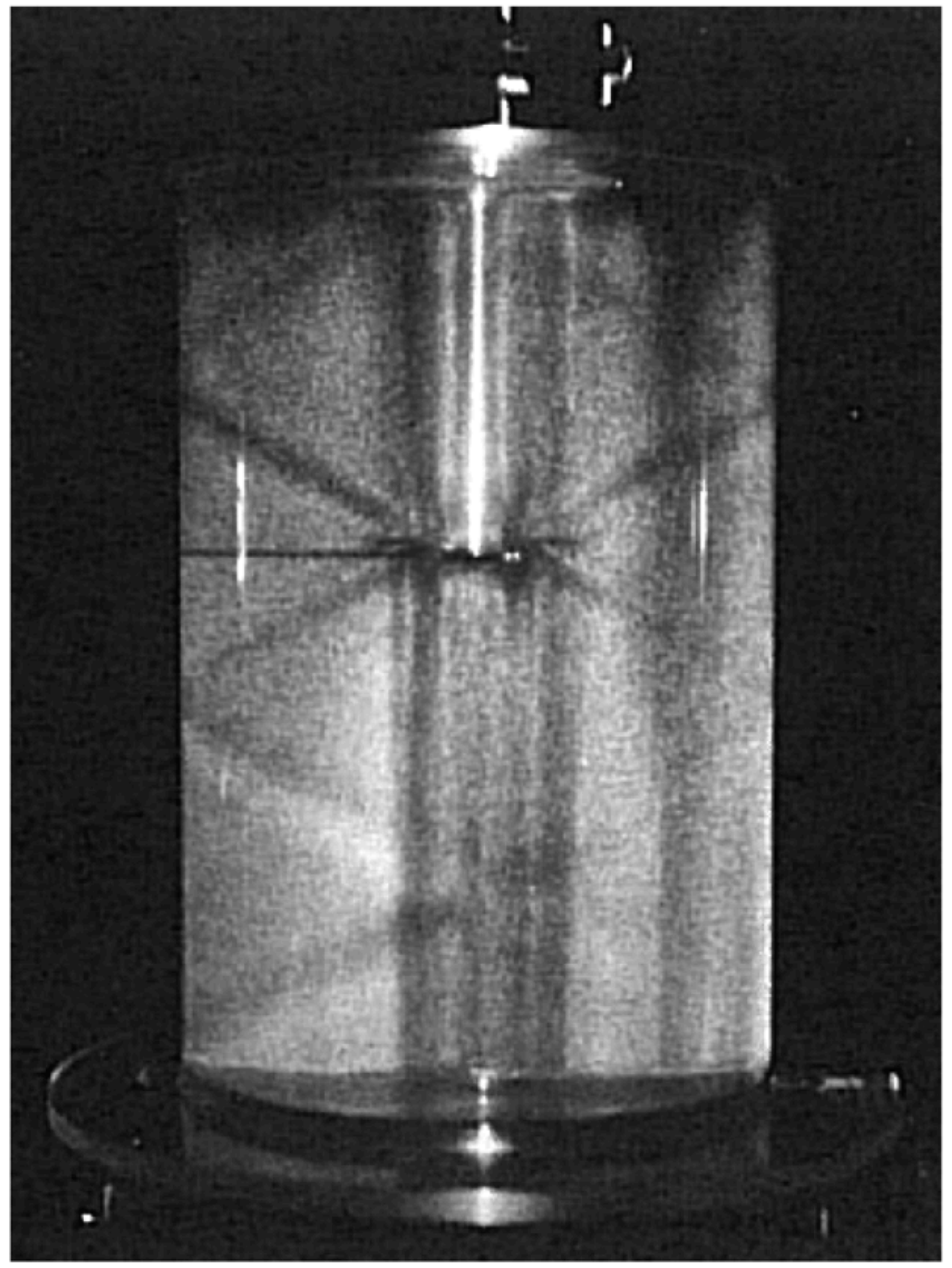

(b)

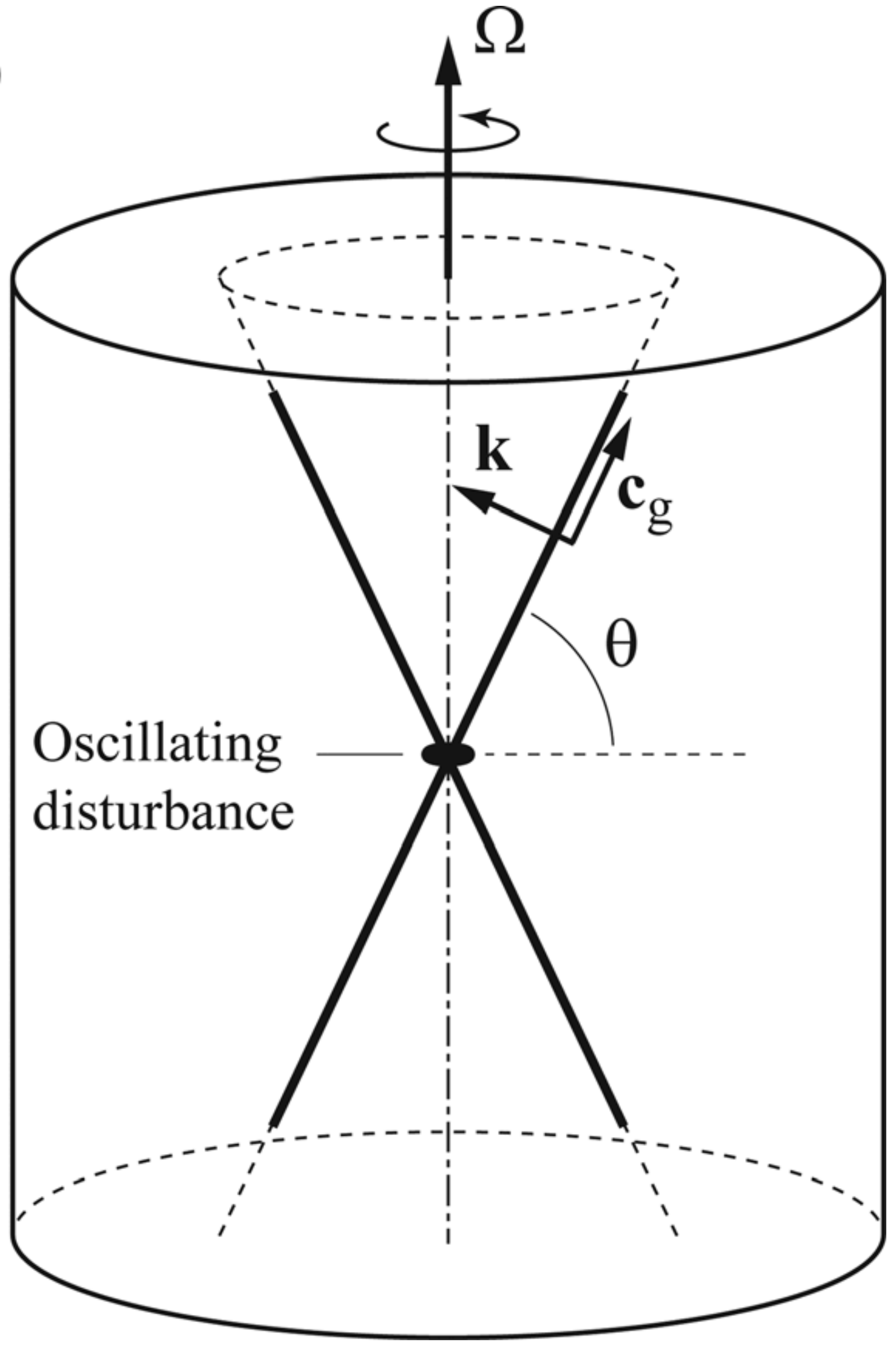

Inertial modes in a rotating shell filled with liquid sodium

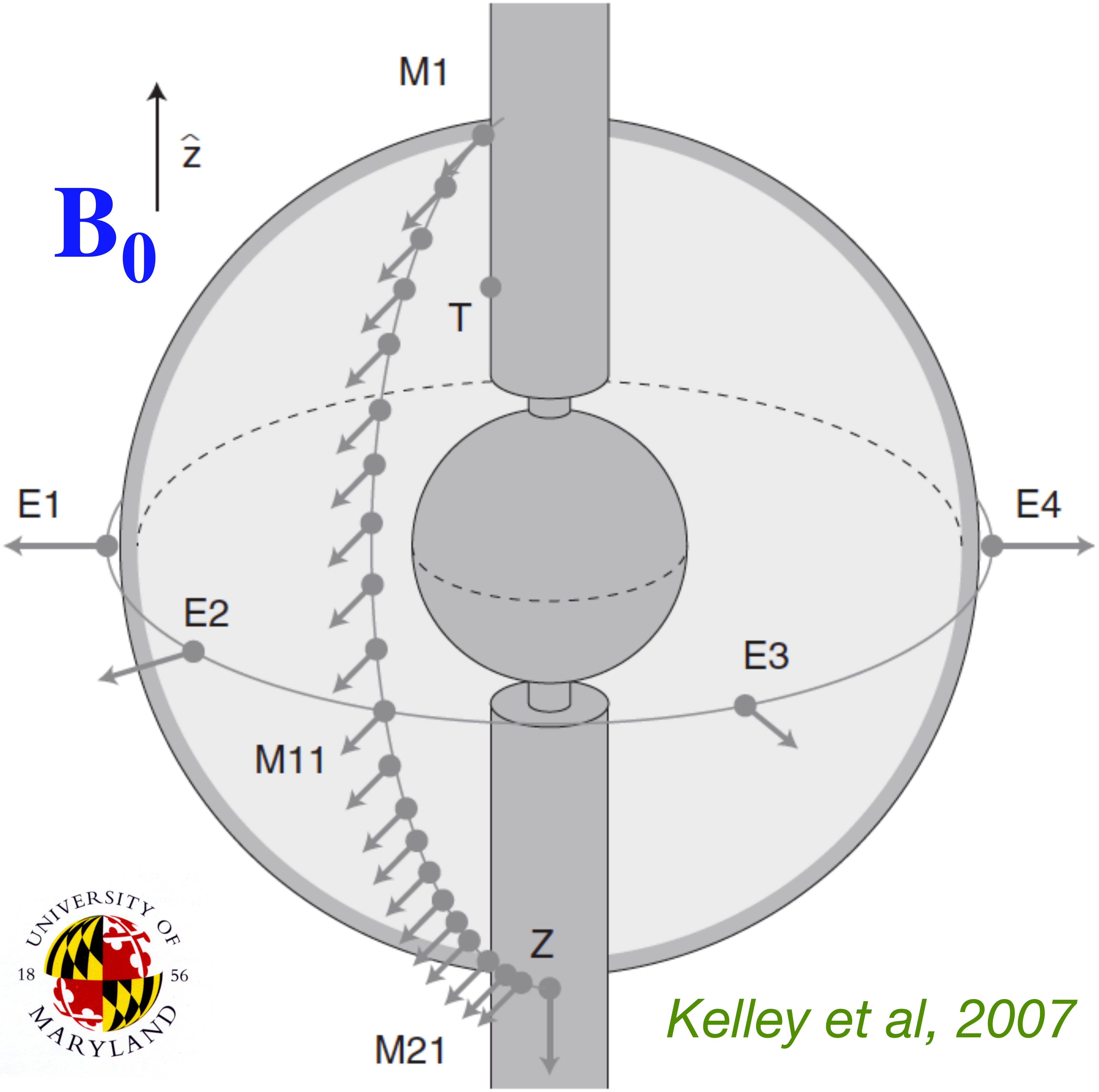

Kelley et al, 2007

- A beautiful demonstration of the presence of inertial modes in a rotating sphere was obtained in an experiment set up in Dan Lathrop's Lab at the University of Maryland.

- A 60 cm-diameter shell holds 110L of liquid sodium (a good electric conductor). A small B_0 magnetic field is imposed.

- Magnetometers along a meridian record the magnetic field induced by inertial modes excited by a differential rotation of the inner sphere.

Inertial modes in a rotating shell filled with liquid sodium

- The video shows the pattern of different inertial modes retrieved from the magnetometers' records, as the differential rotation of the inner sphere is slowly ramped.

- The sound of the video is also built from the magnetometers' records, giving the frequencies of the different inertial modes.

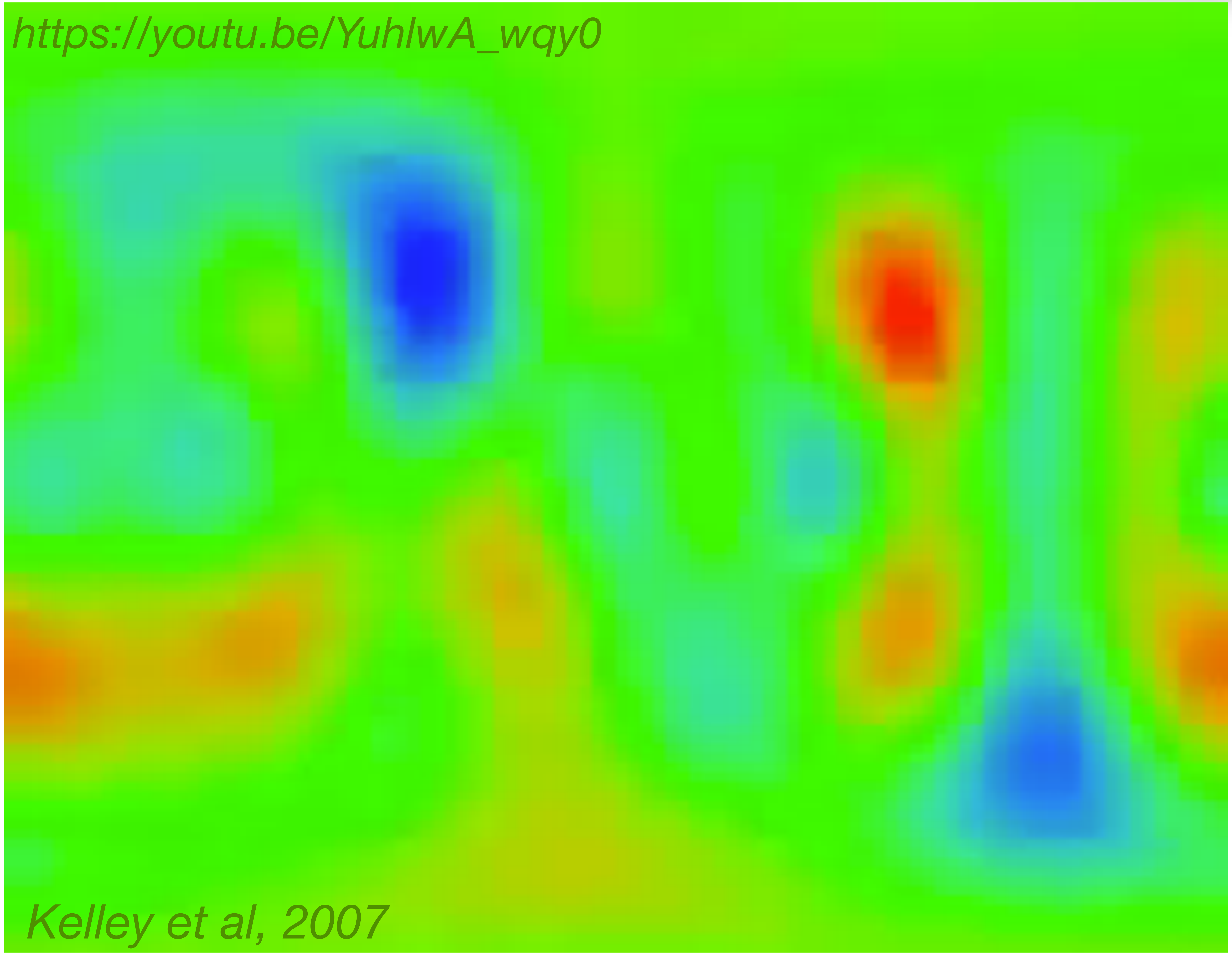

Inertial waves and geostrophic columns

- One crucial role of inertial waves is to build geostrophic (or quasigeostrophic) columns, at a speed $\Omega\ell$ where ℓ is the typical section of the column.

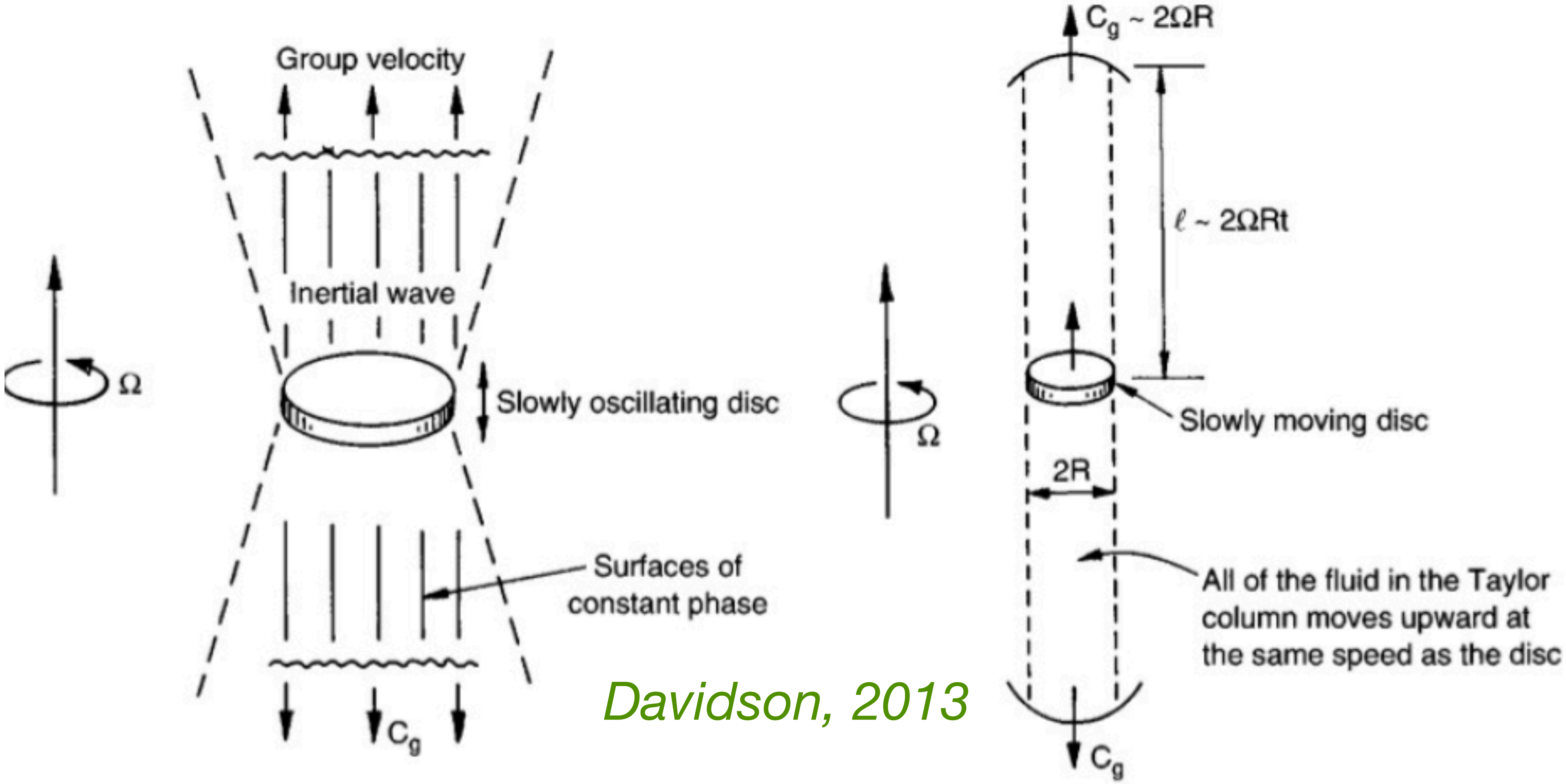

Davidson, 2013

Geostrophic and quasigeostrophic flows in a rotating sphere

- In a rotating sphere, the surface condition implies that the only purely **geostrophic** flows (z-invariant) are **axisymmetric azimuthal flows**.

- If the sphere's surface is a no-slip boundary, there can be no geostrophic flow strictly speaking. However, axisymmetric azimuthal flows can form provided the velocity drop at the surface is accounted for by a thin boundary layer, called the **Ekman layer**.

- Purely azimuthal flows cannot carry heat out of a spherical body. **Quasigeostrophic** flows, which retain a nearly z-invariant structure but allow for non-azimuthal velocities, are the structures that do the job.

3.2.4. Rossby waves

Rossby waves

- Rossby waves are **quasi-geostrophic inertial waves** that feel the **boundaries** of the fluid they travel through. In a spherical container as the core, Rossby waves travel in the prograde direction (eastward), while planetary Rossby waves travel westward in the ocean and atmosphere.

The dispersion relation reads:

$$\omega_{Rossby} = -2\Omega \frac{\beta k_\varphi}{k^2}$$

with $\beta = \dfrac{\alpha}{H_c}$

where α is the slope of the boundary and H_c is the height of the column.

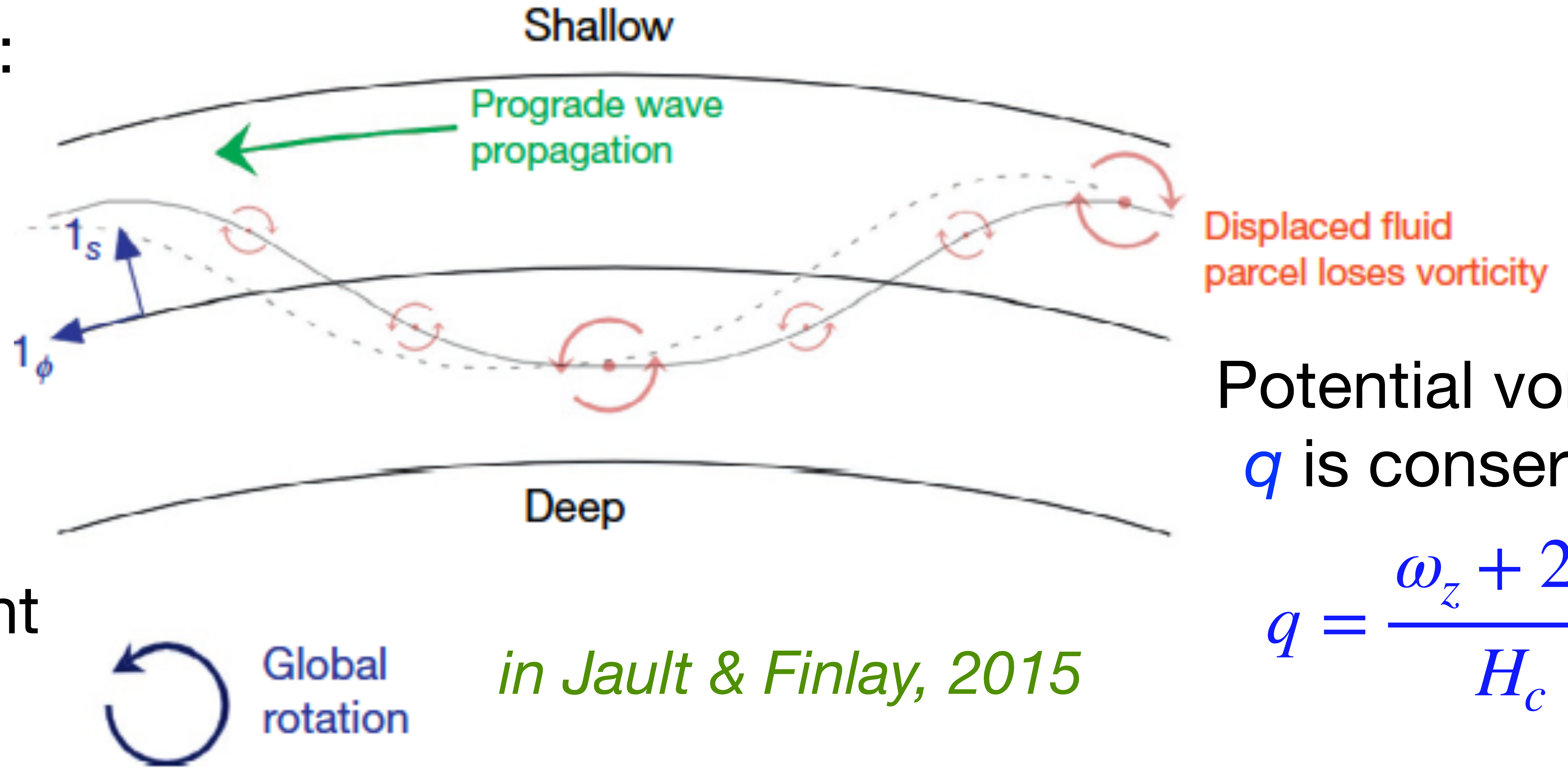

in Jault & Finlay, 2015

Potential vorticy q is conserved

$$q = \frac{\omega_z + 2\Omega}{H_c}$$

NB: magnetic Rossby waves

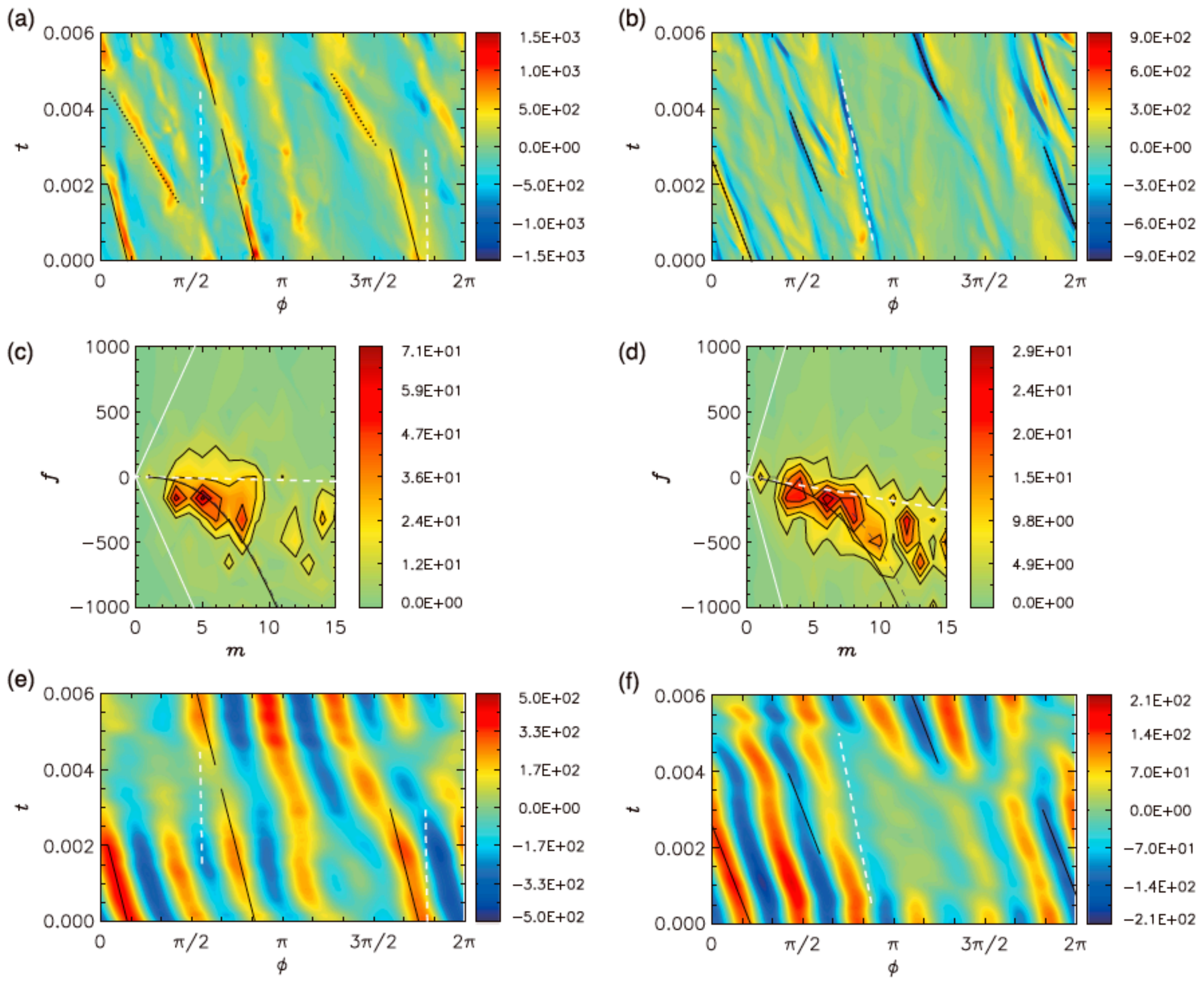

Figure 2. Azimuth time section of $\langle u'_s \rangle$ at (a) $s = 0.5r_o$ and (b) $0.77r_o$ for the run 5R5. White and black lines represent the advective speed due to the mean zonal flow ($\bar{\zeta}$), and the total speed for the slow magnetic Rossby mode ($\bar{\zeta} + \hat{\omega}_{MC}/m$) with different wave numbers m, respectively, at the radii: $m = 5$ (solid) and 8 (dashed) in Figure 2a and $m = 6$ (solid) in Figure 2b. (c and d) Wave number-frequency power spectrum at the same radii. Here white dashed, black dashed, and black solid lines show the advective dispersion relation, $\hat{\omega}_{adv}/2\pi = \bar{\zeta}m/2\pi$, the slow wave ones, $\hat{\omega}_-/2\pi$ (equation (9)), and the total ones, $(\hat{\omega}_{adv} + \hat{\omega}_-)/2\pi$, respectively. The fast mode, $(\hat{\omega}_{adv} + \hat{\omega}_+)/2\pi$, is far beyond the frequency window here. As m is increased, the modes recover the Alfvén waves, whose dispersion relations, $(\hat{\omega}_{adv} \pm \hat{\omega}_M)/2\pi$, are represented by white solid lines. At sufficiently large m, the black solid curve becomes parallel to the white solid line. (e and f) Same as Figures 2a and 2b, but all the wave numbers are filtered out except $m = 4$ to 6 in Figure 2e and $m = 5$ to 7 in Figure 2f.

- (hydrodynamics) Rossby waves should not be mixed up with **magnetic Rossby waves**, which travel westwards.

—> see Kumiko Hori

Hori et al, 2015

3.2.5. Convection in a rotating sphere

Viscosity needed!

- The Proudman-Taylor constraint represents a serious problem for thermal convection! Somehow, it needs to **brake this constraint**, that is to deviate from the geostrophic equilibrium. For that, one of the neglected term in the Navier-Stokes equation should be kept.

- Surprisingly, the best candidate is the **viscous term**! Whereas viscosity inhibits convective instability in the classical Rayleigh-Bénard problem, **viscosity is needed for convection** to start in a rotating sphere.

- This comes at a price: the viscous force has to balance the Coriolis force. This requires shrinking the diameter of convective cells down.

Width of quasigeostrophic columns

- Balancing the Coriolis force by viscous forces in the curled Navier-Stokes equation, we get:

$$2\Omega\,(\hat{\mathbf{z}}\cdot\nabla)\,\mathbf{u} = \nu\nabla\times(\nabla^2\mathbf{u})$$

- If velocity remains almost *z*-invariant, the Coriolis term is of order $\dfrac{\Omega u}{r_o}$,

while the viscous term will depend upon the diameter ℓ of the convective as: $\dfrac{\nu u}{\ell^3}$. Hence: $\ell \sim \left(\dfrac{\nu r_o}{\Omega}\right)^{1/3} = r_o\,E^{1/3}$

Busse columns

- The full theory initiated by Busse (1970) and completed by Jones *et al* (2000) confirms this scaling. It shows that, at threshold, convection takes the form of **thermal Rossby waves**, also called **Busse columns**. It also yields the expression of the critical Rayleigh number Ra_c and associated wave number m_c and frequency ω_c, which are found to vary with the Ekman number E as:

$$Ra_c \sim E^{-4/3}$$

$$m_c \sim E^{-1/3}$$

see Jones, 2015

$$\omega_c \sim E^{-2/3}$$

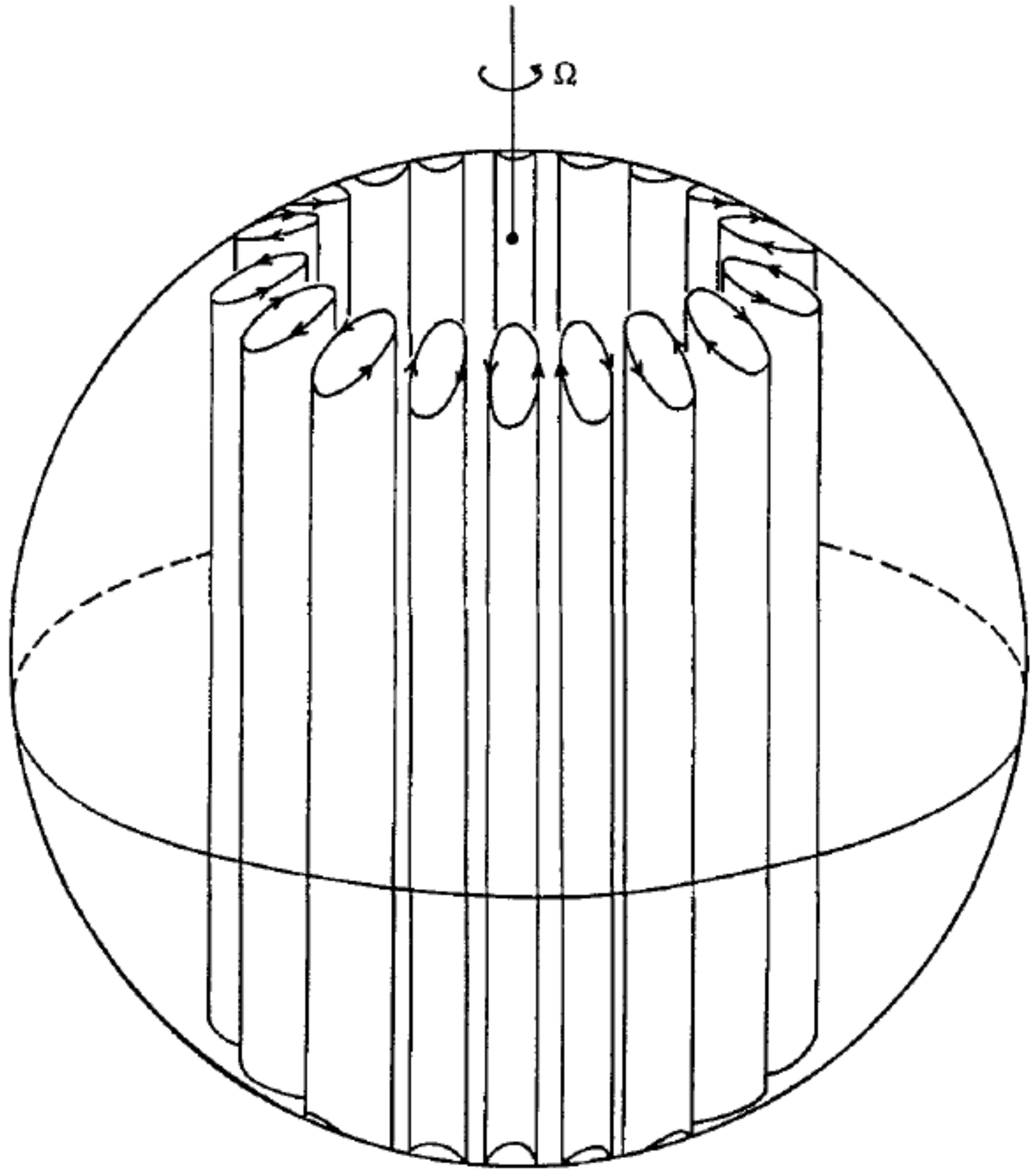

Busse, 1970

… that narrow?

- At this stage, we estimate the diameter expected for these **quasigeostrophic** convective cells at the convection threshold in the Earth's core. We get:

$$\ell \sim r_o E^{1/3} \sim 35\,\mathrm{m}$$

and we usually conclude that it is hard to imagine eddies 35 m in diameter and 3500 km tall…

A recent study by Guervilly et al (2018), backed up by 3D simulations down to $E = 10^{-8}$ and quasigeostrophic 2D simulations down to $E = 10^{-11}$ propose a different scaling, which yields a diameter of about **30 km**.

Quasigeostrophic flow in a numerical simulation of convection

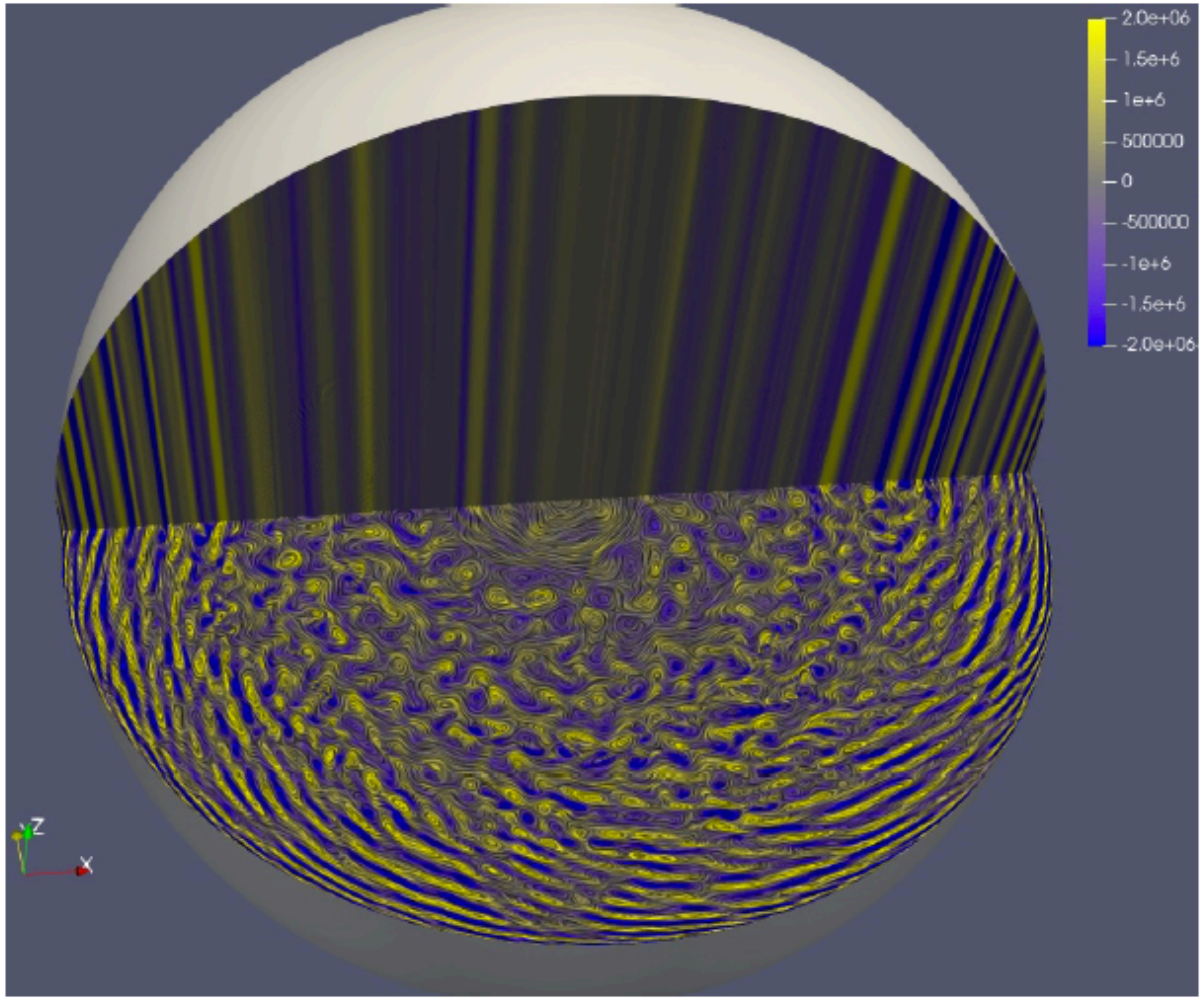

Figure 1: Meridional and equatorial cross-sections of a snapshot of the axial vorticity in the 3D model for $Ek = 10^{-8}$, $Ra = 2 \times 10^{10}$, and $Pr = 10^{-2}$. Streamlines have been superimposed in the equatorial plane. The kinetic energy of the velocity projected on a quasi-geostrophic state $(\langle u_s \rangle, \langle u_\phi \rangle, z\beta \langle u_s \rangle)$ (where the angle brackets denote an axial average) is within 0.2% of the total kinetic energy.

Guervilly et al, 2018

3.3. Dynamos

Outline

3.3. Dynamos

3.3.1. Larmor and Bullard’s disk dynamo

- In a very short note, Joseph **Larmor** proposed in 1919 that the magnetic field of the Sun, and incidentally of the Earth, could be produced by **dynamo action**.

- Years later, Ed **Bullard** proposed a simple thought experiment to illustrate this principle: the **homopolar disk dynamo**.

Joseph Larmor
1857-1942

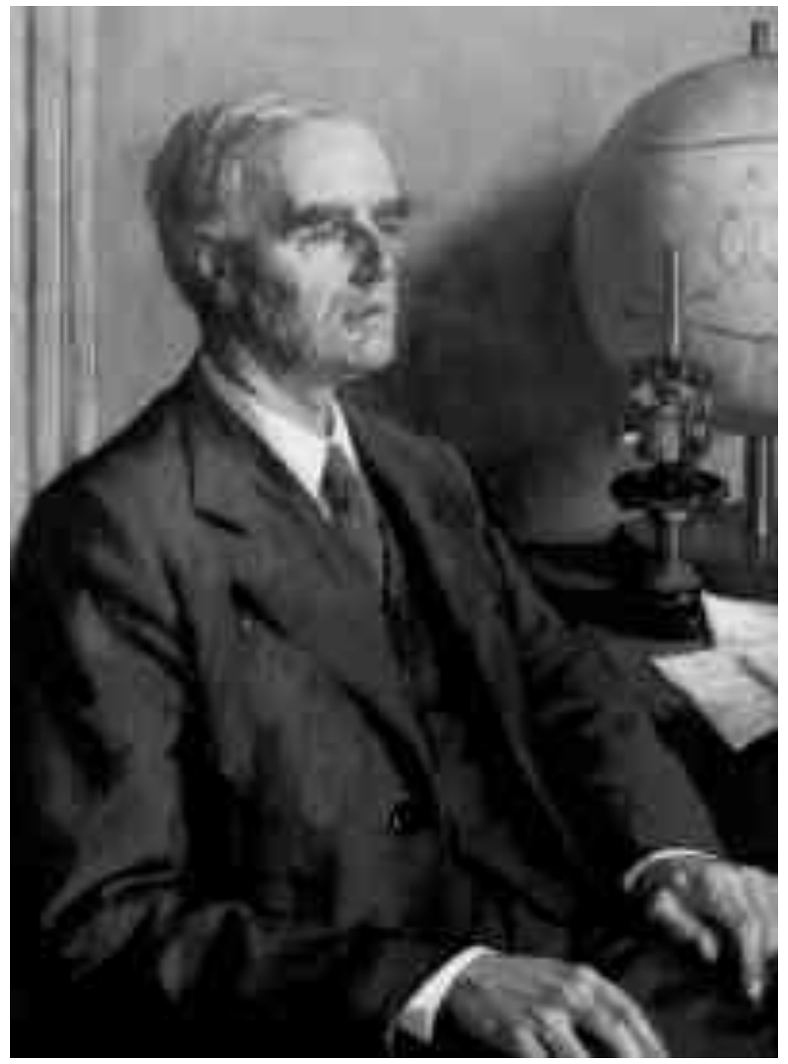

Edward Bullard
1907-1980

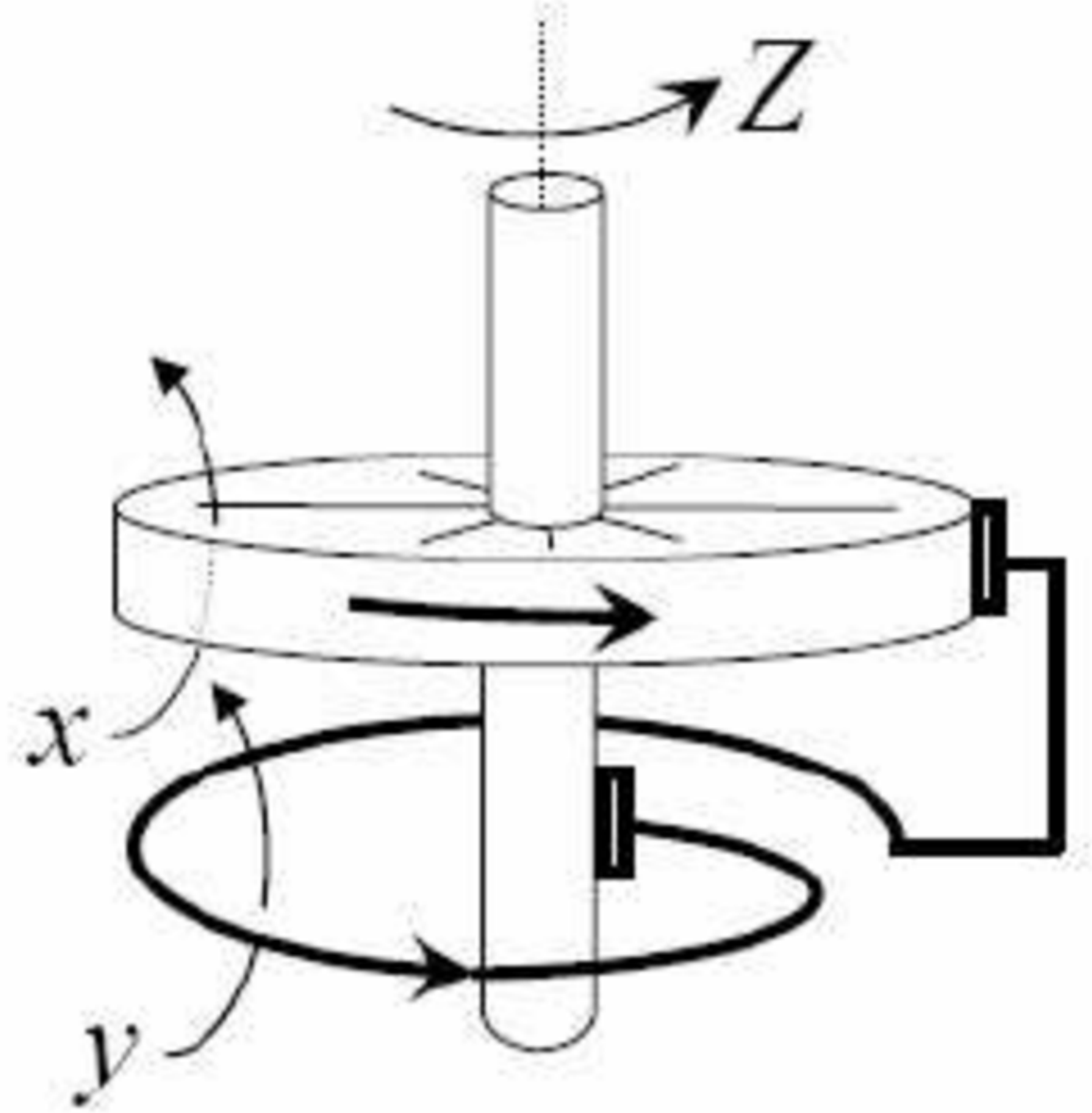

3.3.2. Cowling's theorem

Kinematic dynamo

- The magnetic induction equation looks very simple: $\frac{\partial \mathbf{B}}{\partial t} = \underbrace{\nabla \times (\mathbf{u} \times \mathbf{B})}_{induction} + \underbrace{\eta \nabla^2 \mathbf{B}}_{diffusion}$

- The first question one might ask is: given a velocity field **u**, can a magnetic field **B** grow. This is called the **kinematic dynamo** problem.

- Given some characteristic velocity *U* and dimension *L* of the system, a first answer comes from comparing induction to diffusion as given by the magnetic Reynolds number:

$$Rm = \frac{UL}{\eta}$$

- The magnetic Reynolds number must be large enough for dynamo action to occur. However, not all velocity fields qualify!

Cowling's theorem

- In 1934, Thomas Cowling demonstrated a theorem stating that **no purely *axisymmetric* magnetic field can be maintained by dynamo action**. This shed some doubts upon the validity of this mechanism for explaining natural dynamos.

- Therefore, many theoretical and experimental efforts were devoted to finding a solution to this problem.

« It was the Larmor theory ultimately that I was criticizing »

Thomas Cowling, AIP interview, 1978.

Cowling's theorem

- Let's see the essence of Cowling's theorem.

- We define a velocity field **u** and a magnetic field **B**. Both fields are solenoidal (divergence-free). They can be decomposed into a **poloidal** component and a **toroidal** component.

- We consider magnetic induction in a sphere, and assume that both fields are **axisymmetric**. We can then write:

$$\mathbf{B} = \mathbf{B_P} + B_\varphi \hat{e}_\varphi \quad \text{with} \quad \mathbf{B_P} = \nabla \times (A\hat{e}_\varphi)$$

$$\mathbf{u} = \mathbf{u_P} + s\,\omega\,\hat{e}_\varphi$$

where A, B and ω (fluid angular velocity) are scalar fields, and s is the cylindrical radius.

Cowling's theorem

- The induction equation then becomes:

$$\begin{cases} \dfrac{\partial A}{\partial t} = \eta \Delta_1 A - \dfrac{\mathbf{u_P}}{s} \cdot \nabla (sA) \\ \dfrac{\partial B_\varphi}{\partial t} = \eta \Delta_1 B_\varphi - s\mathbf{u_P} \cdot \nabla \left(\dfrac{B_\varphi}{s} \right) + s\mathbf{B_P} \cdot \nabla \omega \end{cases} \quad \text{with} \quad \Delta_1 \equiv \nabla^2 - \frac{1}{s^2}$$

- These equations show that the velocity field can produce some toroidal magnetic field B_ϕ by shearing the poloidal field $\mathbf{B_P}$: this is the **omega effect.**

- However, the scalar A of poloidal magnetic field cannot draw energy from the B_ϕ field. Hence no dynamo: this is **Cowling's theorem**.

3.3.3. Mean field summary

Mean field

- One way out of Cowling's theorem is to allow for small **non-axisymmetric fluctuations** around the mean axisymmetric fields. One writes:

$$\mathbf{B} = \langle \mathbf{B} \rangle + \tilde{\mathbf{b}}$$

$$\mathbf{u} = \langle \mathbf{u} \rangle + \tilde{\mathbf{u}}$$

- The induction equation for the mean axisymmetric magnetic field then becomes:

$$\begin{cases} \dfrac{\partial A}{\partial t} = \eta \Delta_1 A - \dfrac{\mathbf{u_P}}{s} \cdot \nabla (sA) + \mathscr{E}_\varphi \\ \dfrac{\partial B_\varphi}{\partial t} = \eta \Delta_1 B_\varphi - s\mathbf{u_P} \cdot \nabla \left(\dfrac{B_\varphi}{s} \right) + s\mathbf{B_P} \cdot \nabla \omega + \left[\nabla \times \mathscr{E} \right]_\varphi \end{cases}$$

Mean field kinematic dynamos

- The mean of the $\mathbf{u} \times \mathbf{B}$ product contains an additional **electromotive force** $\mathscr{E}$, which is the contribution of the cross-term of the fluctuations to the mean induction:

$$\mathscr{E} = \langle \tilde{\mathbf{u}} \times \tilde{\mathbf{b}} \rangle$$

- In some conditions, the electromotive force can be expressed as:

$$\mathscr{E} = \alpha \langle \mathbf{B} \rangle - \beta \nabla \times \langle \mathbf{B} \rangle$$

- This led to the very successful development of **mean-field** $\alpha\omega$ **kinematic dynamos**, which played a large role in deciphering the magnetic field of the Sun and the solar cycle.

3.3.4. Experimental dynamos

- Experimental dynamos were built to address some key issues, which evolved in time.

- The first attempts aimed at showing the reality of dynamo action, and rested on geometries that were supposed to yield a dynamo.

- Such experiments are difficult: the best liquid electric conductor known (liquid sodium) has a magnetic diffusivity **η = 0.1 m²/s**. In order to reach a value of the magnetic Reynolds of order **100**, an experiment must have dimensions in the **meter range** and fluid velocities in the **10 m/s range**.

$$Rm = \frac{UL}{\eta} \sim \frac{10 \times 1}{0.1} \sim 100$$

Lowes and Wilkinson

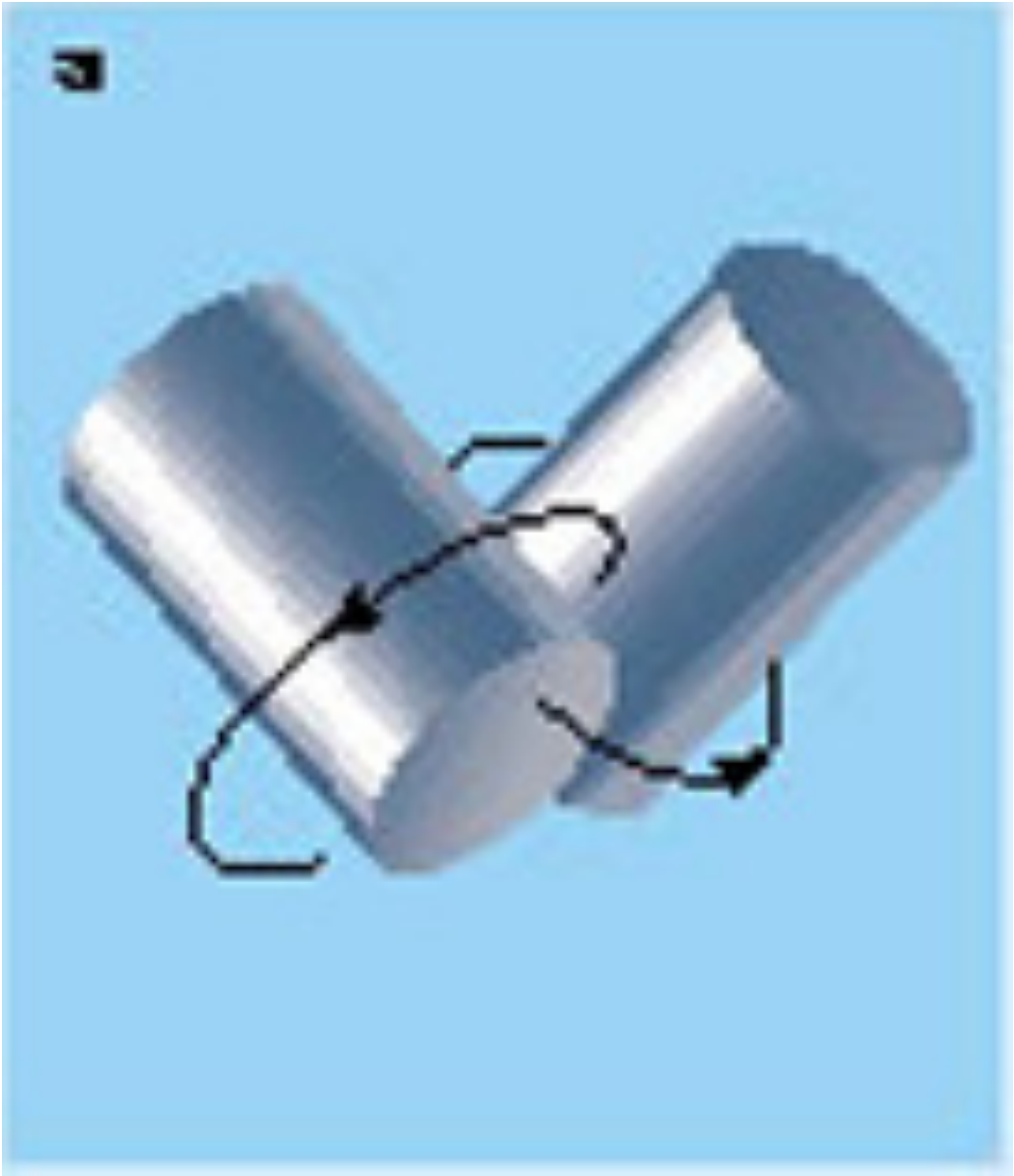

- The first experiment, due to **Lowes and Wilkinson** (1963; 1968) was inspired from the **Herzenberg** geometry (1958).

- The experiment consisted in two rotating cylinders embedded in a block of **ferromagnetic** iron (to decrease the magnetic diffusivity). Electric contact was ensured by liquid mercury.

- After some efforts, the experiment **did produce a magnetic field**. **Reversals** were observed in some cases.

Karlsruhe liquid sodium dynamo

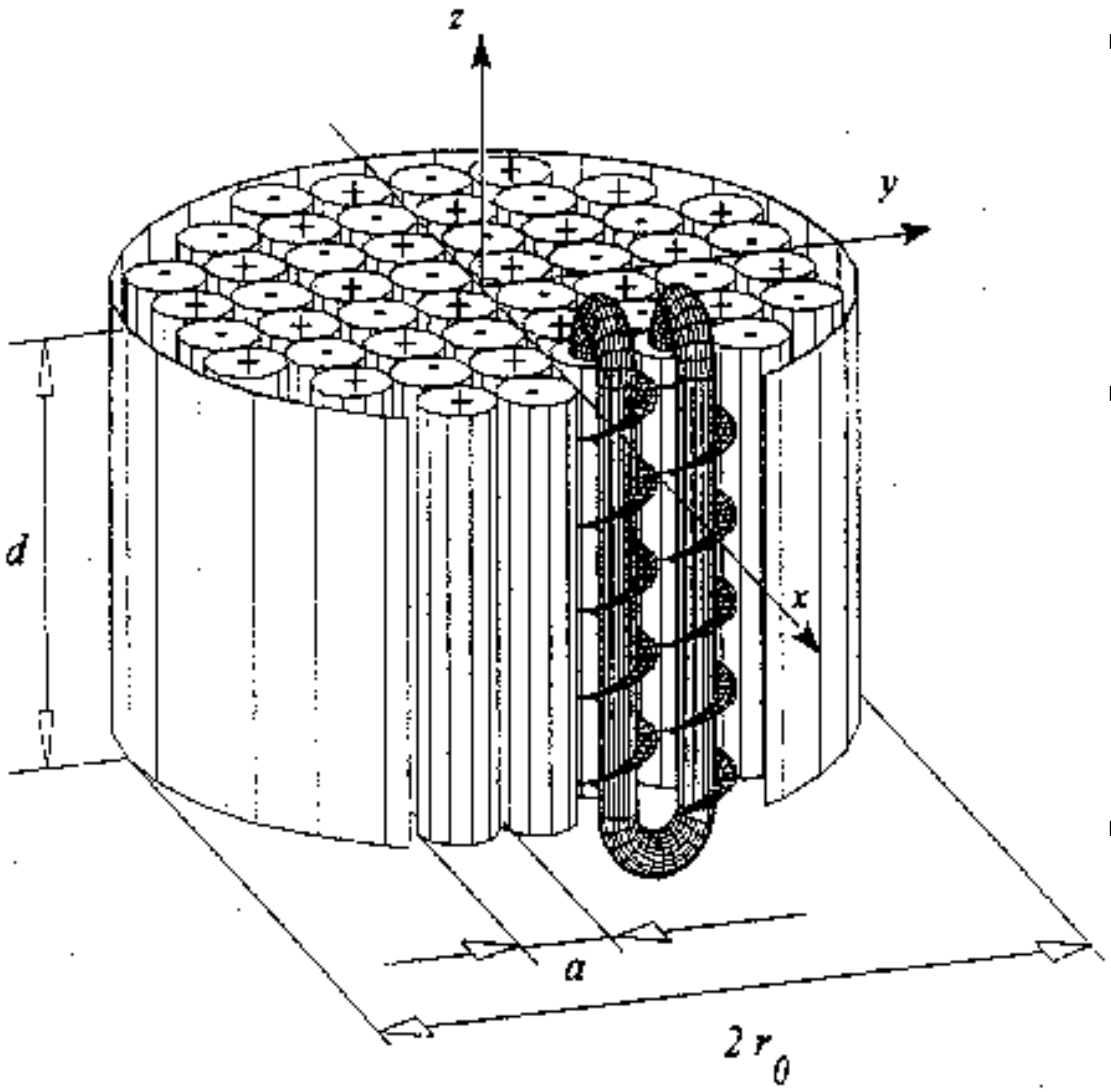

- The Karlsruhe liquid sodium dynamo experiment was built by **Müller and Stieglitz**, following the design of **G.O. Roberts** (1972).

- **Liquid sodium** is forced into pipes that pave a large cylinder. In year 2000, a magnetic field was produced, with the expected geometry.

- This experiment demonstrated the **validity** of the effect of **scale-separation**, assumed in mean-field theories.

- In year 2000 as well, after years of efforts, **Agris Gailitis** and his colleagues got the **Riga liquid sodium** experiment become a dynamo.
- The design follows a proposal by **Ponomarenko** (1973). The dynamo onset and the geometry of the magnetic field were in agreement with the predictions.
- This dynamo gives much **more freedom** to the flow, with turbulent fluctuations around 10%. The **saturation** of the magnetic field is due to the braking effect of the Lorentz force on the swirling flow.

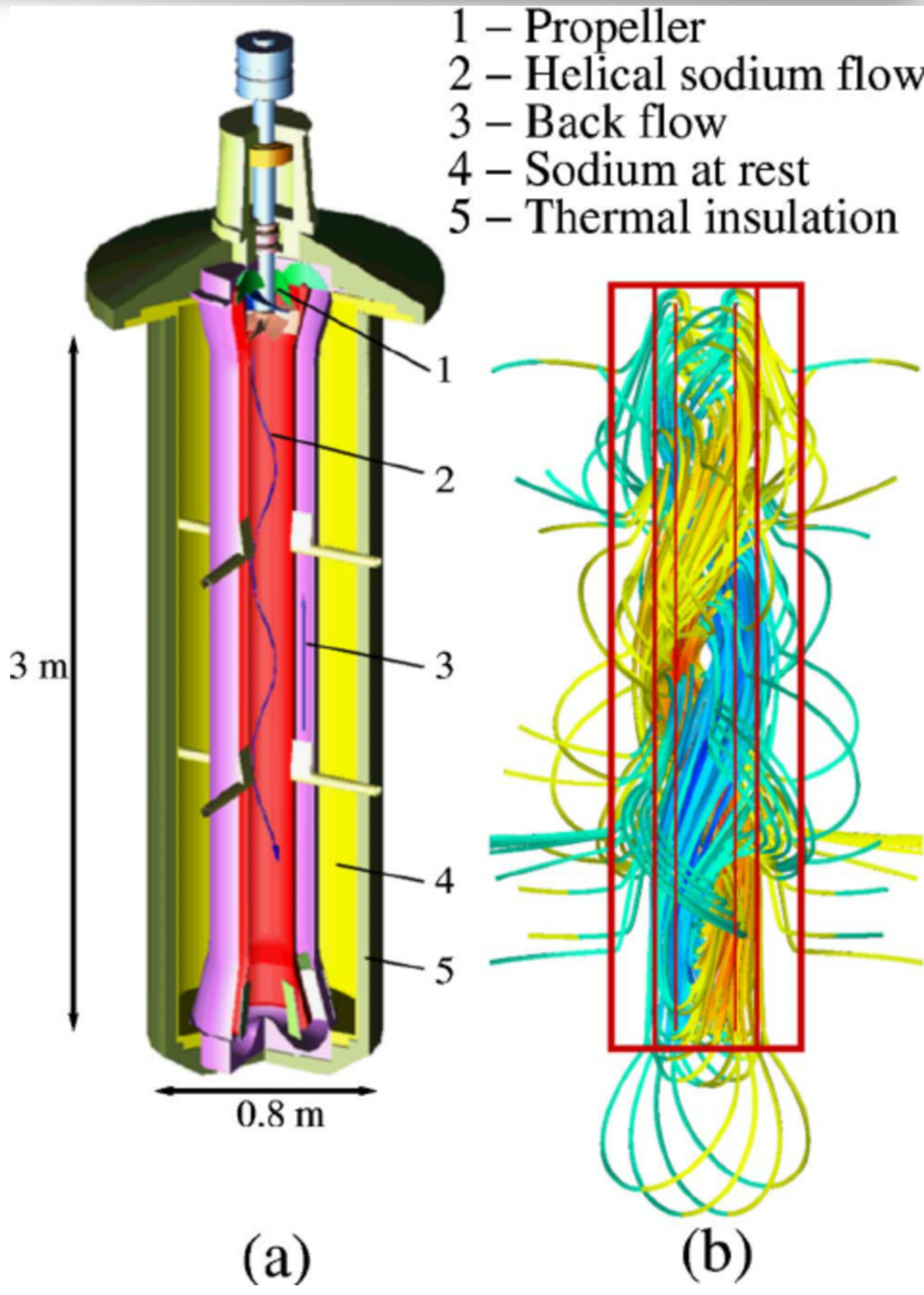

Second generation experiments

- After the success of the Riga and Karlsruhe dynamo experiments, it was felt that experiments were needed with **less constrained flows**, possibly closer to natural situations.

- This meant an additional complexity: since the magnetic Prandtl number of liquid sodium is

$$Pm = \frac{\nu}{\eta} \simeq 7.3 \times 10^{-6}$$

  in order to reach magnetic Reynolds number values of order 100 requires reaching kinetic **Reynolds number of order 10 millions**, *i.e.* a very turbulent flow.

- Several teams engaged in this adventure. All met a similar problem: turbulent fluctuations appear to **change the geometry of the magnetic field** the experiment can produce, and more annoying, to **increase the critical value**.

Cary Forest's experiment in Madison

- The liquid sodium experiment of Cary Foret's team, at the University of Wisconsin generates a **very turbulent** swirling flow in a 1 m-diameter sphere. It did not reach self-excitation, but showed that the **fastest growing magnetic mode** was **axisymmetric** around the rotation axes, in contrast with the predictions based on the mean flow.

Spence et al, 2006

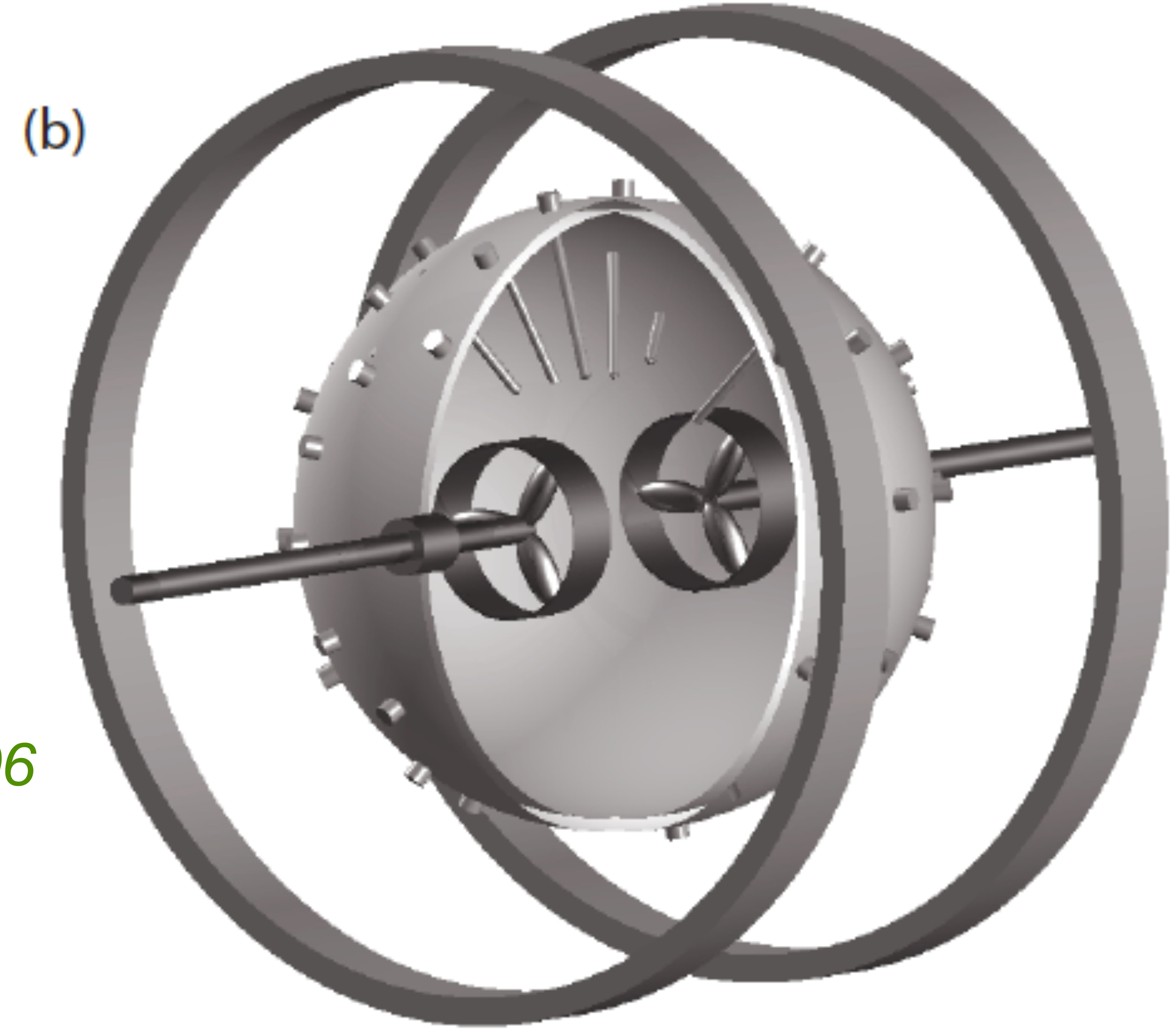

The Cadarache VKS experiment

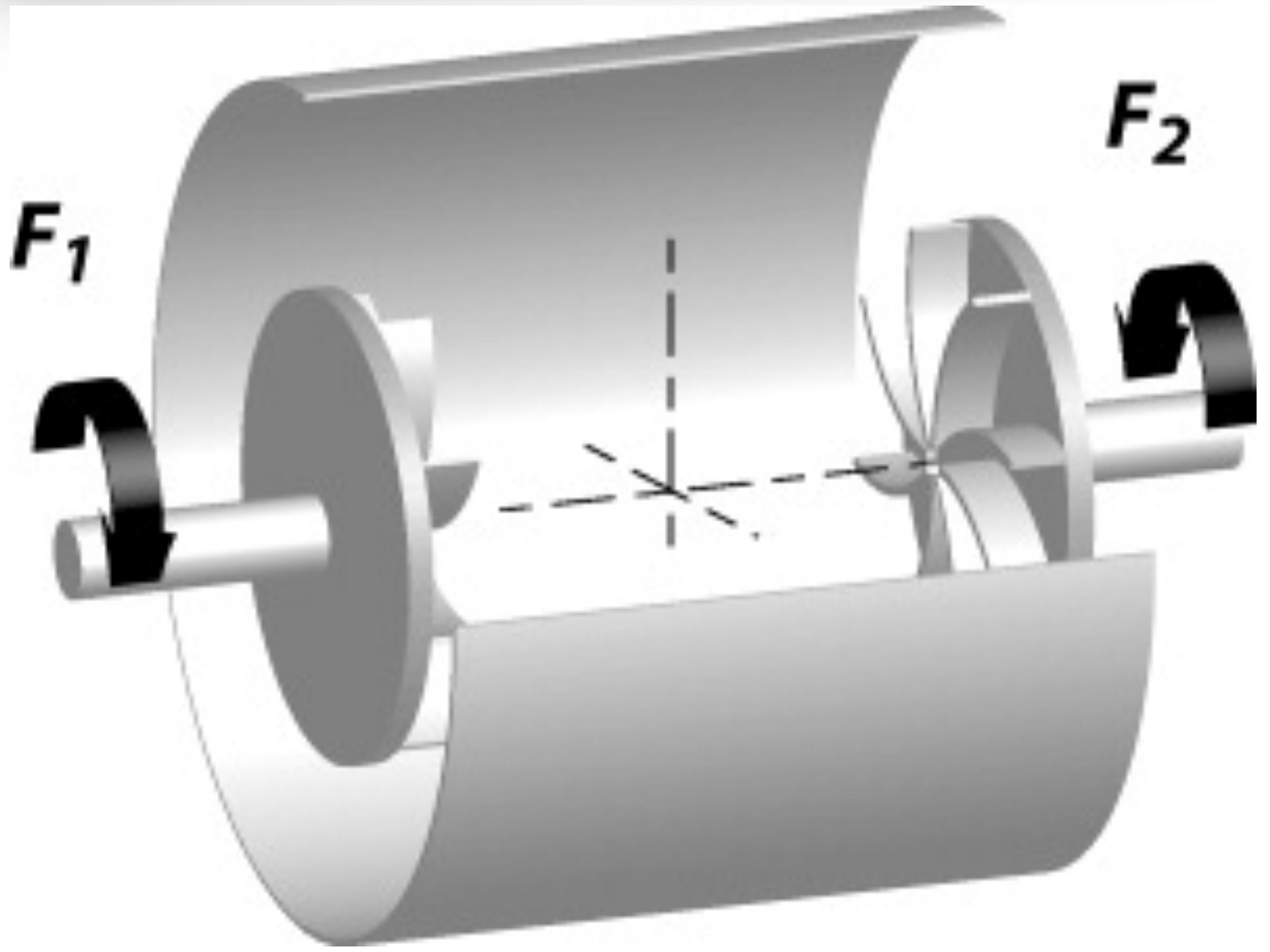

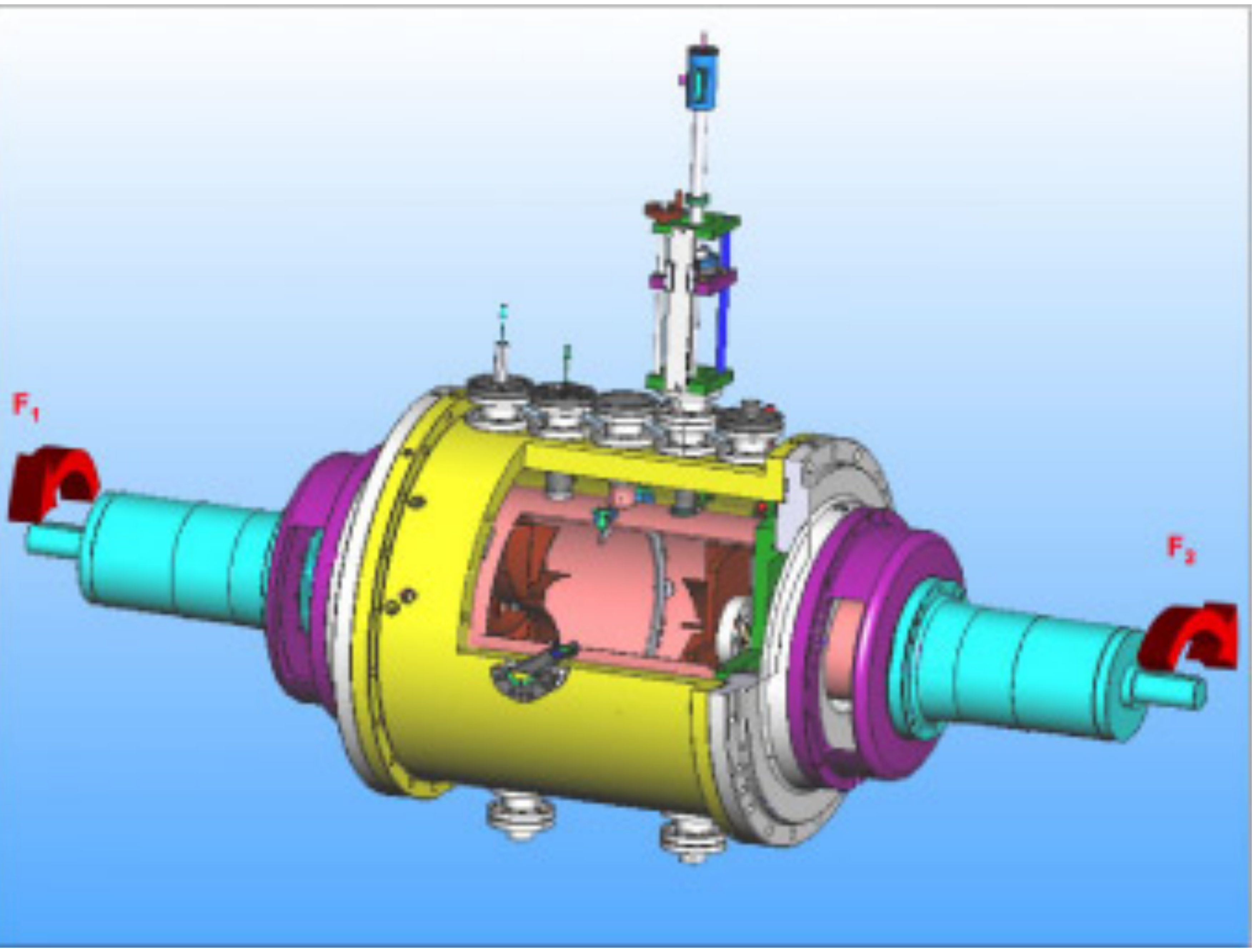

- The VKS experiment generates a **very turbulent Von Karman** swirling flow. The experiment was designed to reach the dynamo threshold as estimated from the mean flow. No magnetic field was produced at this value.

- However, **dynamo action was observed** after replacing one or both rotating disk by a **soft iron disk** (Monchaux et al, 2007). The produced magnetic field was then mostly azimuthal and **axisymmetric**, in contrast with the expectation from the mean flow.

- **Beautiful magnetic reversals** are observed when the disks don't spin at the same rate (Berhanu et al, 2007).

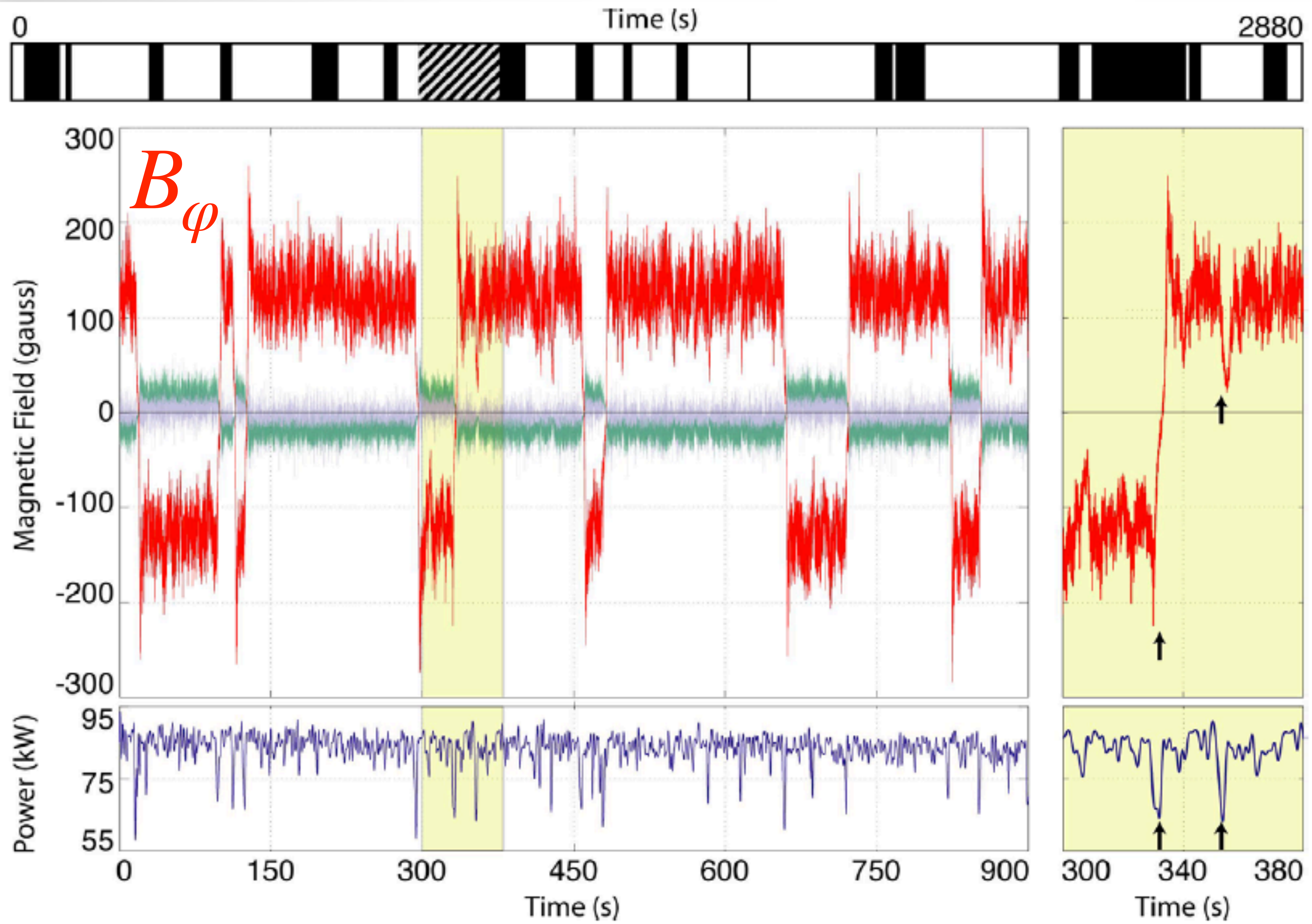

- Series of magnetic field reversals in the VKS dynamo experiment.

Berhanu et al, 2007

Dan Lathrop's dynamo experiment at U Maryland

- Probably the most ambitious experiment was set up by Dan Lathrop and his team at the University of Maryland. The 3 m-diameter sphere holds **12 tons of liquid sodium!** It can spin around a vertical axis, and holds an inner sphere that can also spin around the same axis.

- In contrast with other experiments, the entrainment of the liquid is only by friction with the smooth inner sphere. For that reason, although the experiment could in principle reach values of the **magnetic Reynolds number** as high as **900**, it did not self-excite.

Dan Lathrop's dynamo experiment at U Maryland

In action at its maximum rotation frequency of **3.95 Hz**!

A test performed with the water-filled experiment.

Dan Lathrop's dynamo experiment at U Maryland

Although it did not reach self-excitation, the experiment produced interesting **magnetic bursts**, which seemed to **enhance** an applied magnetic field.

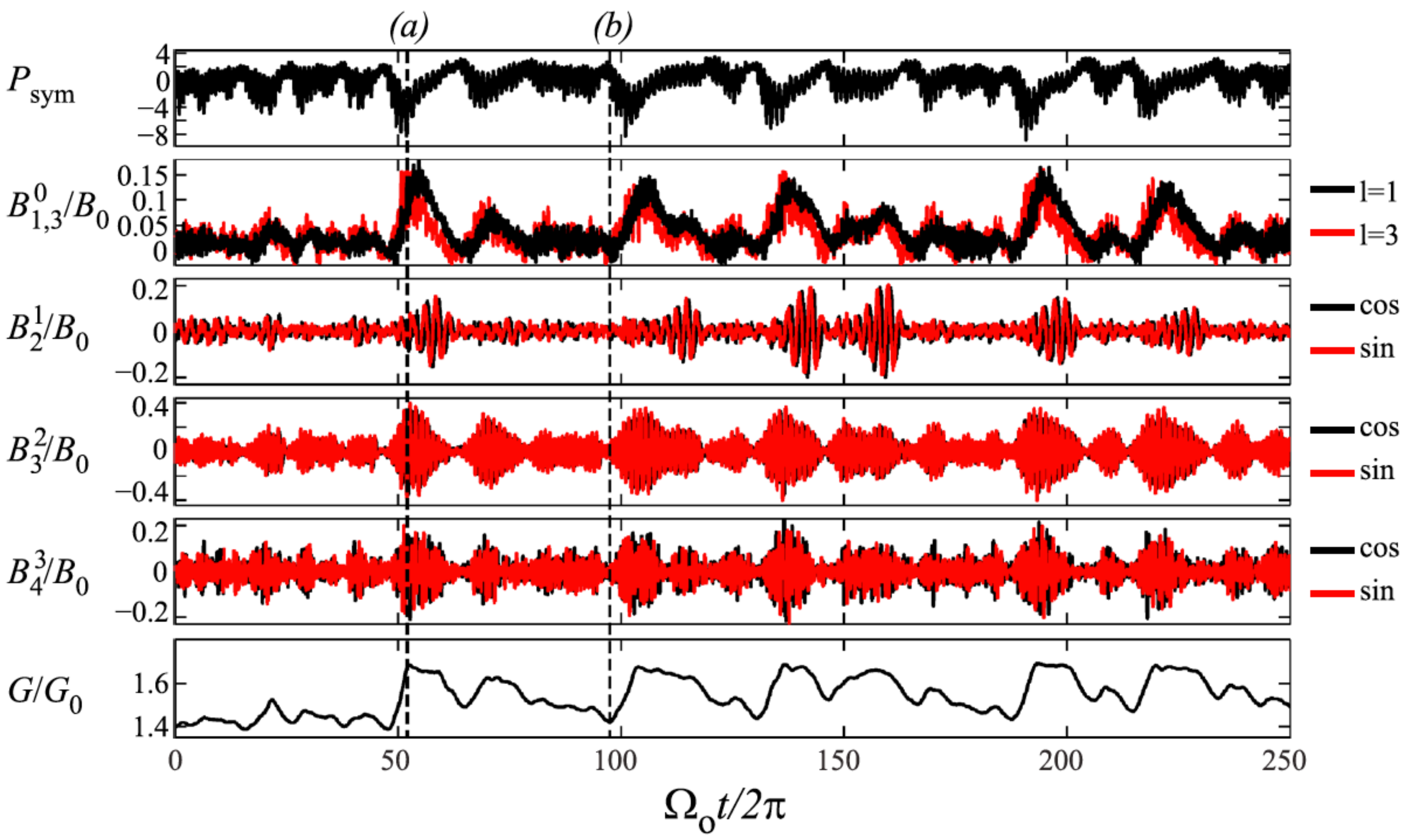

Dan Lathrop's dynamo experiment at U Maryland

- The geometry of Dan Lathrop's experiment, inspired from the Earth's core, is very close to that of the (much smaller) **DTS experiment** developed in Grenoble.

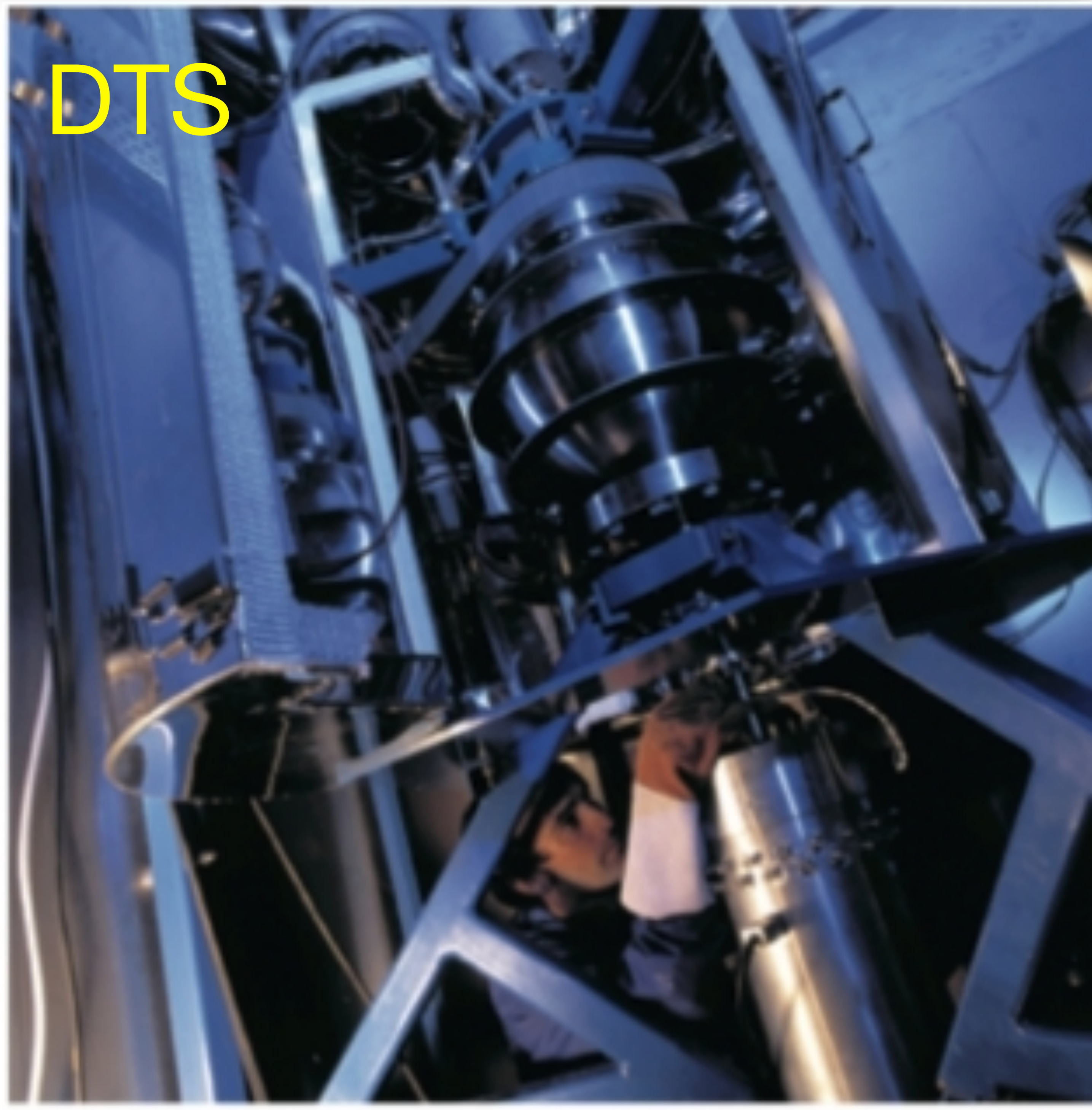

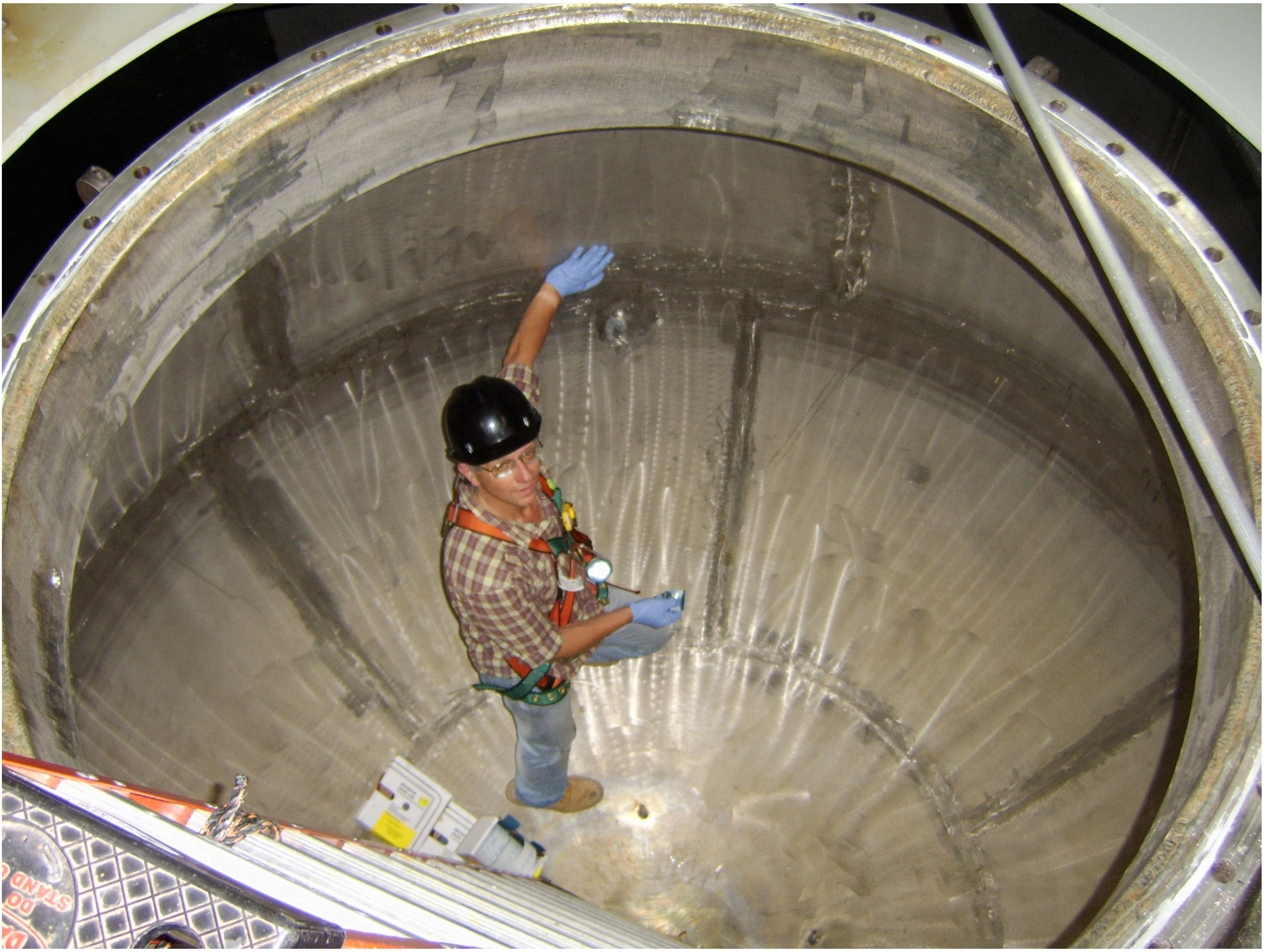

- I had the chance to spend some time at the University of Maryland and take part to some of the preparatory work on the 3m experiment.

A precession-driven dynamo experiment in Dresden

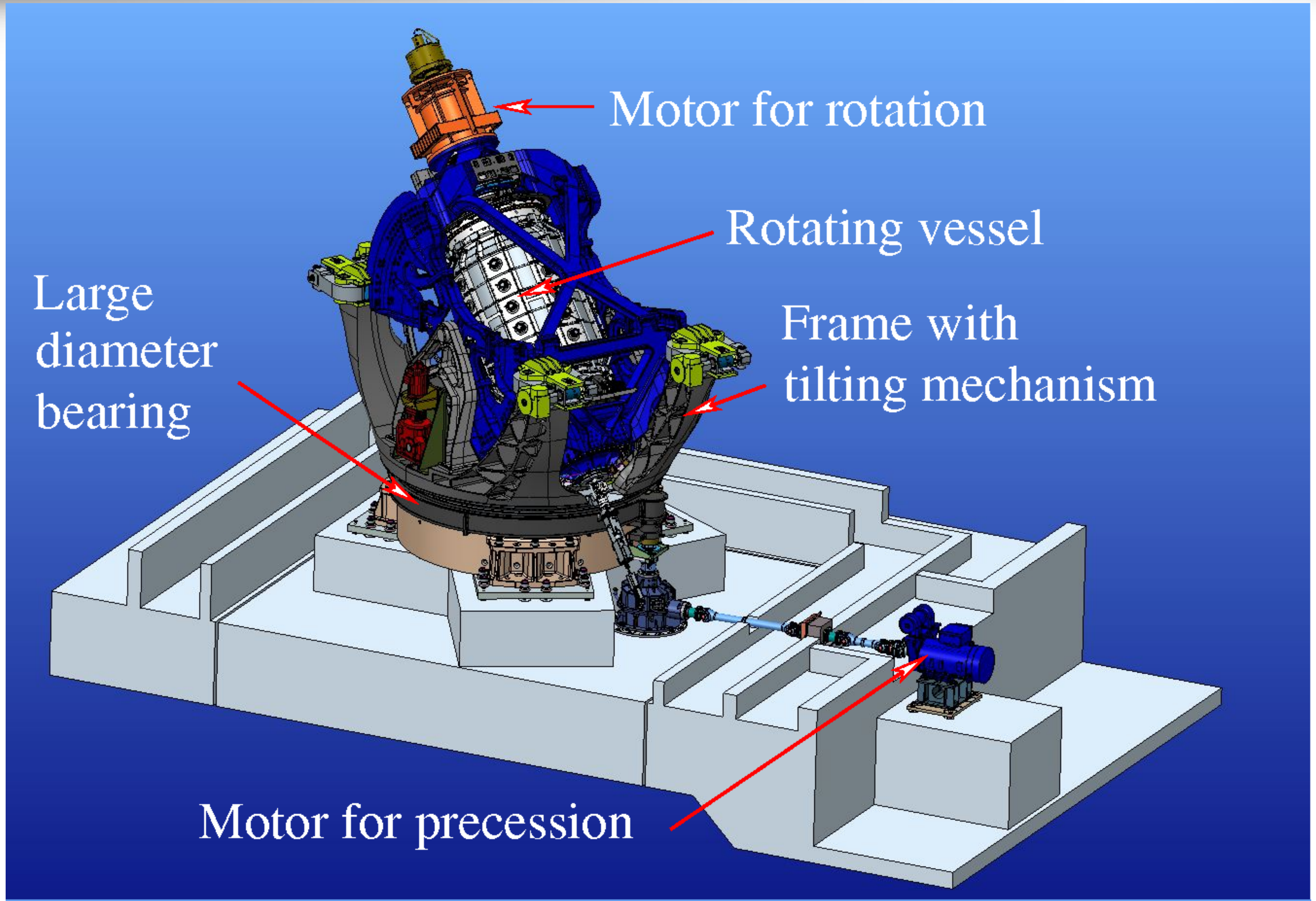

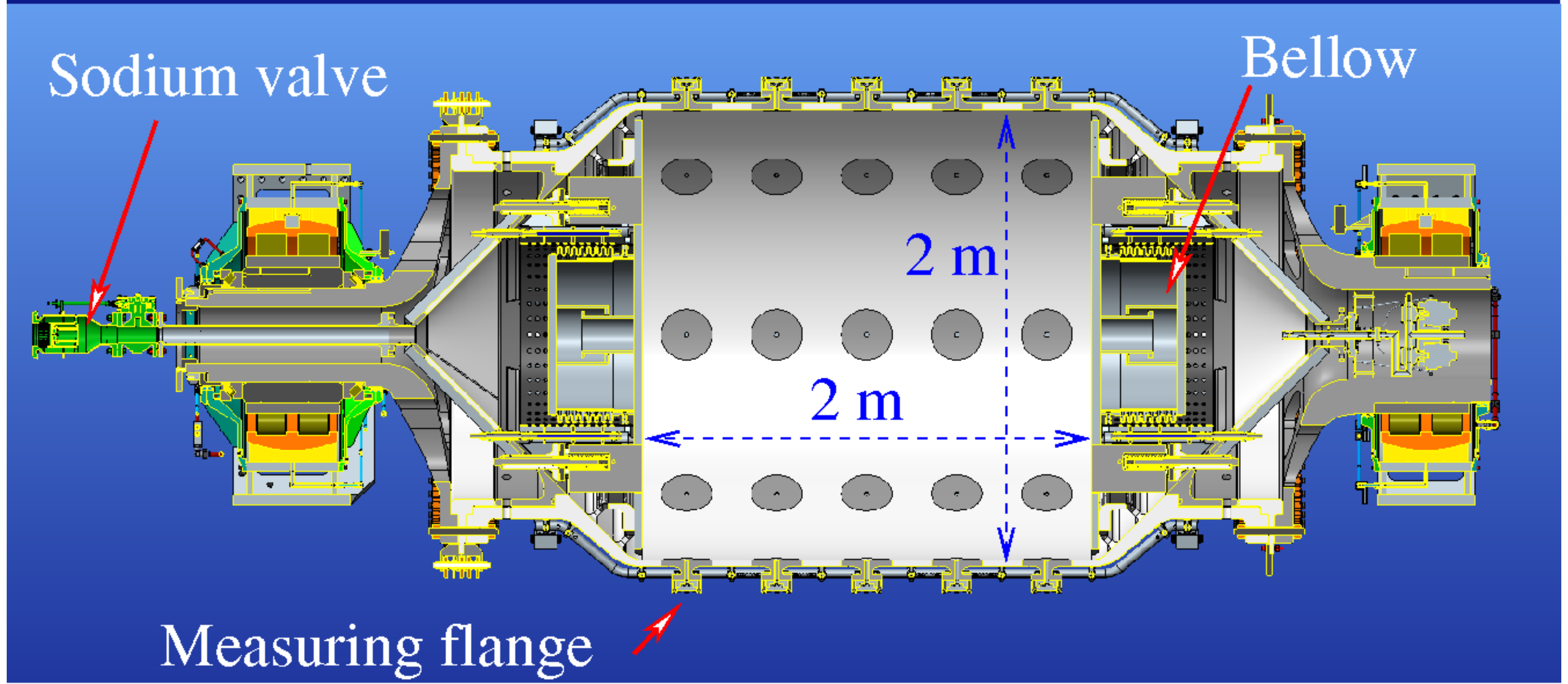

- An even more ambitious dynamo experiment is under construction in Dresden, under the supervision of Frank Stefani.
- The driving is by **precession**, a mechanism that is a candidate for explaining the strong ancient magnetic field of the Moon.

Dynamo experiments: pros and cons

- Very small magnetic Prandtl number, as in planetary cores.
- Can be observed over very long times (overturn and magnetic diffusion time).
- Ground truth test of our theories.
- Force reasoning with real systems.
- Unexpected observations trigger new developments.

- Difficult, expensive, and dangerous.
- Little hope for a convective experimental dynamo.
- Magnetic energy only a few percents of the kinetic energy.
- Lack fundamental ingredients of natural dynamos.
- Results difficult to compare with observations.